acp-2016-365

Schmidt et al., On-line single particle analysis of ice particle residuals from mountain-top mixed-phase clouds using laboratory derived particle type assignment

Reply to Reviewer #1

Reviewer comments and questions are printed in this font type.

Our replies are printed like this.

Changes to the manuscript text are printed in green.

General comments:
The manuscript by Schmidt et al. presents valuable measurements of single-particle mass spectra from ice clouds, focusing on the composition of ice residual particles (IPR) in mixed-phase clouds. The manuscript is well formatted and presents a valuable experiment. Given the rarity of such measurements and the apparent success of the experiment, which was a difficult and complex one, the manuscript is appropriate for publication in ACP. This manuscript is also important for having attempted a direct laboratory confirmation of each particle class.

Thank you for this positive rating.

Major comments:
1-
The first question that comes to mind while reading this paper is the uncertainty of all reported values. Some effort was made for Fig. 3 but not for the clustering results. Roth et al. (2016, by the same group) describe a procedure to estimate uncertainties for these clustering results, why was this not applied here? If the authors have a good reason for not adapting the Roth 2016 method, and I realize some adaptation would be necessary, then they should use some other approach to numerically report their best estimated clustering uncertainties.
Clustering uncertainties should also be combined (eg in quadrature) with Poisson based sampling uncertainties to take sampling times into account. With these two sources of statistical uncertainty addressed, perhaps some of the rarer classes in Figs 2 and 6 may fall below the method limit of quantification.
Other uncertainties to be discussed include the % of laboratory particles that did not show the marker peaks and potential cross sensitivity of different marker peaks.
After uncertainties are estimated each stated percentage value % should include an uncertainty, for example those stated in Section 3.2.2.

We added an error estimation following the method described in Roth et al (2016).

The method is based on a manual inspection of a subset of the data. The assignment of a certain cluster to a particle type is based on the presence of the reference marker peaks in the averaged cluster mass spectrum. Upon inspection of all mass spectra in one cluster it may occur that the marker peaks (or not all of the marker peaks) are not present in an individual

mass spectrum. Such a mass spectrum has nevertheless been correctly (from a mathematical point of view) assigned to the cluster by the algorithm, because the overall correlation of the mass spectrum with the cluster average is sufficiently high ($r > 0.7$). This can especially occur in cases when many other peaks are similar, as is often observed for organic particles.

For the error estimation, such particle mass spectra were regarded as "uncertain assignments". The percentage of such uncertainly assigned mass spectra was regarded as the relative error and was generalized to the whole data set.

Of the out-of-cloud data set we inspected two clusters, one assigned to biological particles (338 particles) and one that was assigned to biomass burning aerosol (473 particles). It turned out that 52 of the 338 "biological" mass spectra were uncertain (15%), and 48 of the 473 "biomass burning" mass spectra (10%). Thus, we conservatively estimated the relative error for the out-of-cloud aerosol to be about 15%.

Of the IPR data set, where the absolute numbers of particles are much lower, it was possible to do a more detailed inspection of the clusters: We inspected one cluster assigned to biological particles, where we found that 28 out of 76 were uncertain (37%), and one cluster of the "PAH/soot" particle type, where 9 out of 23 spectra were uncertain (40%). Those particle types containing only a small number of particles ("industrial metals", "Na + K", "aged material") were completely inspected manually, yielding uncertainties for the "industrial metals" of 14%, of the "Na + K" type of 0% (no uncertain particles), and of the "aged material" type of 44%.

Thus, we estimated the relative error (from uncertain particle type assignment) of the IPR population to be 40% with the exception of the industrial metals (14%) and the "Na + K" type.

These error estimates are conservative upper limits for the error range, because the reference laboratory measurements have shown that, e.g., not all biological particles contain the characteristic marker peaks. It may therefore well be that mass spectra that are similar to the cluster average spectrum of a "biological particle" type are really biological particles, even if they do not contain the marker peaks.

For the total error, this relative error was combined with the Poisson statistic error (by error propagation) of each particle type. The error ranges were added to Figure 2 (previously Fig. 1) and Figure 7 (previously Fig. 6) and in the text in all cases where the relative abundance of particles is mentioned.

The description of the error estimation given above was added to the text of the manuscript (section 2.2):

The uncertainties reported along with these numbers were estimated by manual inspection of a subset of the data, as described in Roth et al. (2016). The assignment of a certain cluster to a particle type is based on the presence of the reference marker peaks in the averaged cluster mass spectrum. Upon inspection of all mass spectra in one cluster it may occur that the marker peaks (or not all of the marker peaks) are not present in an individual mass spectrum. Such a mass spectrum has nevertheless been correctly (from a mathematical point of view) assigned to the cluster by the algorithm, because the overall correlation of the mass spectrum with the

cluster average is sufficiently high (r > 0.7). This can especially occur in cases when many other peaks are similar, as is often observed for organic particles.

For the error estimation, such particle mass spectra were regarded as "uncertain assignments". The percentage of such uncertainly assigned mass spectra was regarded as the relative error. Of the out-of-cloud data set we inspected two clusters, one assigned to biological particles (338 particles) and one assigned to biomass burning aerosol (473 particles). It turned out that 52 of the 338 inspected "biological" mass spectra (15%), and 48 of the 473 inspected "biomass burning" mass spectra (10%) had to be considered as uncertain. Thus, we conservatively estimated the relative error to be about 15% and generalized this error for whole out-of-cloud data set.

For the IPR data set, where the absolute numbers of particles are much lower, it was possible to do a more detailed inspection of the clusters: We inspected one cluster assigned to biological particles, where we found that 28 out of 76 were uncertain (37%), and one cluster of the "PAH/soot" particle type, where 9 out of 23 spectra were uncertain (40%). Those particle types containing only a small number of particles ("industrial metals", "Na + K", "aged material") were completely inspected manually, yielding uncertainties for the "industrial metals" of 14%, of the "Na + K" type of 0% (no uncertain particles), and of the "aged material" type of 44%. Thus, we estimated the relative error (from uncertain particle type assignment) of the IPR population to be 40% with the exception of the industrial metals (14%) and the "Na + K" type.

These error estimates are conservative upper limits for the error range, because the reference laboratory measurements have shown that, e.g., not all biological particles contain the characteristic marker peaks. It may therefore well be that mass spectra that are similar to the cluster average spectrum of a "biological particle" type are really biological particles, even if they do not contain the marker peaks. The uncertainty inferred from manual inspection was combined with the Poisson counting statistics error (by error propagation) for each particle type.

2-

What makes this paper special compared to other single-particle mass spec papers is the laboratory study of different particle types. Section 2.3. This must have taken a significant effort, and is well motivated. Therefore, the laboratory results should be published in full detail!

Average mass spectra for each particle type, including error bars, could be added. These could be added in the supplement and also placed next to the identified particle types in Figure 1.

We decided to add the mass spectra of the reference particle to the supplement. Placing them in Figure 1 is not ideal, because there is usually more than one cluster for each reference particle type and we would like to show these different clusters.

Changes to text:

The laboratory reference mass spectra are shown in the supplement (Figures S1 through S20). It was found that one reference particle type produced several types of spectra which were separated using the clustering algorithm described above. The supplement lists the main clusters with the number of spectra in each cluster.

The authors suggest that marker ions may be instrument specific. However, the importance or unimportance of this variability is unknown until multiple labs publish such data. Moreover, I do not see why such markers should be instrument specific if all variables (eg laser wavelength, fluence, and pulse duration) are controlled. LDI mass spectrometry databases do exist outside of aerosol science.

We agree, if all parameters were controlled and identical, marker ions should not be instrument specific. However, custom built instruments (like our ALABAMA) have different geometries and optical components than others, such that even when the same laser type is used, the energy density at the point of particle ablation may be different. Also the broadening of the particle beam (different aerodynamic lenses, difference flight path lengths) and thereby the variation of the ablation point, and also the acceptance region of the mass spectrometer itself (extraction voltages may be different) are not the same in different instruments. Thus, to our opinion there are many reasons why these marker ions are instrument specific, and care should be taken when using our reference mass spectra for other instruments.

3-
In Section 2.3 when discussing the lab spectra it is stated "only those mass spectra that represented the majority of the different fragmentation patterns were considered". What % defines majority? Moreover, this % should be used to define a correction factor (with corresponding uncertainty propagated into the result). If only 60% of particles were measured for salt but 90% for soot, then the reported IPR numbers should be scaled up by 1/0.6 and 1/0.9 respectively.

In the supplement we show the mass spectra types (clusters) from each reference particle type along with the percentages.

Correction of the reported IPR numbers can't be done in this way. First, we might end up with more particles that were actually measured. Second, it is only possible to assign marker ions of atmospheric particles to those reference spectra containing these marker ions. Speculating about spectra not containing the markers would only increase the uncertainty.

4-
Table 1 means nothing to the reader who has not read Roth (2014), since none of the parameters were defined or explained. Roth (2014) is a PhD thesis in German, and is therefore not accessible to the general community. I have quickly looked at the other publication by Roth et al. (2016) and it looks like a great deal of effort was put into the clustering algorithm, including uncertainty consideration. So it is a pity if the reader of the present manuscript does not know that.
Could the authors please include uncertainty analysis of the clustering results in this manuscript. Also a brief description of the conceptual basis of the chosen clustering algorithm and corresponding uncertainty are missing from Section 2.2 (p4,3).

We removed Table 1 and included the information into the text, describing the meaning of each parameter. Also, we added a general explanation of the clustering and of the chosen algorithm to section 2.2.:

Basically, a clustering algorithm tries to find the optimum number of clusters (i.e. groups of mass spectra) that represent the particle population by their average mass spectrum. By nature of the aerosol particle diversity and the non-uniform ionization in laser ablation ionization, it can't be expected that all particles contained in a cluster equal the average cluster spectrum (Hinz et al., 1999). Rather, each spectrum is assigned to that cluster where the distance metric (in our case one minus Pearson's correlation coefficient r) of the single particle spectrum and the averaged cluster spectrum reaches a minimum. The fuzzy c-means algorithm differs from the k-means in that way that it accounts for the possibility that one particle may belong to two (or more) clusters by using membership coefficients, whereas the k-means assigns each spectrum strictly to that cluster where correlation with the averaged spectrum is highest.

Here we applied the fuzzy c-means algorithm because sensitivity tests conducted in the framework of a PhD thesis (Roth, 2014) with laboratory-generated particle of known composition and number have shown that the fuzzy c-means better separates the particle types and suffers less from false assignments. Also, various parameters that influence the clustering result where tested by Roth (2014), resulting in a "best choice" that was applied here as well: All mass spectra were normalized to reduce the influence of total signal intensity, and all m/z peaks were taken to the power of 0.5 to reduce the influence of the non-uniform laser ablation ionization, thereby increasing the influence of smaller peaks and decreasing that of larger signals. The "fuzzifier", a weighting exponent used for the calculation of the membership coefficients (Bezdek, 1982; Roth et al., 2016) was set to 1.2. A high number of start clusters was chosen to assure that also rare spectra types are considered in the data evaluation (for instance for the out-of-cloud data set from the JFJ campaign 2013 a number of 200 cluster was chosen; for a known particle composition as sampled during the laboratory studies a number of 10 to 50 cluster was chosen depending on the number of spectra). The start clusters were chosen randomly from the total particle population, under the condition that the correlation coefficient (r) between two randomly picked start spectra is less than 0.7. The procedure leading from the clustering algorithm to a certain number of particle types, as illustrated in Figure 1, was as follows: After mass calibration, the spectra were clustered using the fuzzy c-means algorithm, yielding a certain number of clusters. The resulting cluster number can be lower than the chosen number of start clusters. If this is the case, the number of start clusters was sufficiently high not to suppress rare spectra types. Each cluster includes a certain number (≥ 1) of mass spectra based on the calculated membership and distance. From all mass spectra in a cluster an average spectrum is calculated which is used for the identification of the particle type represented by each cluster. All mass spectra which did not fulfill the distance criterion ($1 - r \leq 0.3$) compared to any of the clusters were sorted in the cluster "others". The averaged spectra of each cluster were manually examined with respect to the presence of the marker peaks derived from the reference mass spectra (Section 3.1) and assigned to a certain particle type. The "others" cluster was processed again using the fuzzy c-means algorithm, but with reduced constraints and again the resulting clusters were manually examined and, if possible, assigned to particle types. At the end all clusters of the same particle type were merged, whereas clusters that could not be assigned to a certain particle type were added to the cluster "others".

We added the uncertainty discussion (as already mentioned above) to section 2.2.

Finally, this manuscript used the name "rest cluster" whereas Roth et al. (2016) used the name "others cluster". I find the name "rest" confusing because this word has multiple meanings. "Others" has only one..

We changed the name from “rest” to “others”.

5-
I have several comments about the marker peaks and particle types:

5a- Although the general principle of finding unique marker ions is valid, I cannot see from the manuscript how the marker ion approach was possible. On p7,2 the text states that Table 3 contains "specific" marker peaks, but since these peaks overlap in almost all cases they are not specific. A step by step explanation of how these markers were applied is necessary to understand what was done. A flow chart would be helpful.

The expression "specific" was misleading. We should better have used "characteristic" and we changed it in the manuscript. The combination of these peaks was found to be characteristic for the particle class (first column in Table 3). See also reply to comment 5b.

We also added a flow chart (Figure 1), explaining the procedure in more detail.

5b- It would be a great improvement to split the marker peaks in Table 3 into two subtypes, one containing marker peaks that are truly specific and allowed unambiguous identification of a particle type, and the other containing marker peaks that provide supporting information. Please also clarify the meaning of the colors in Table 3. The caption says that red colors are specific to each type, but this is not true, e.g. minerals and desert dust and volcano dust all share peak 27. Bacteria and pollen share 71. etc.

Marker peaks that unambiguously identify a certain particle type are very rare. Typically we find a combination of peaks that is characteristic to a certain particle type or particle class. As stated above, we replaced "specific" by "characteristic". The combination of the colored peaks in Table 3 is used to assign a mass spectrum to a certain particle type or particle class.

5c- Cn peaks are present in cigarette smoke, fuel exhaust, soot, desert dust, volcano dust. So which peaks were used as markers to distinguish these classes? Were the minor differences in the Cn range really enough to distinguish these types? This is connected to the previous point.

This is a good example to explain the procedure. First, it has to be emphasized again that the identification of particle types for the Jungfraujoch can only rely on the cations.

Desert dust and soil dust contain Fe^+ (m/z 56), the combustion related particles don't. By this, we can separate the mineral particles from the combustion particles.

Cigarette smoke, fuel exhaust, and soot are indeed very similar. But soot particles have a large C_n chain (as shown in Table 3: up to C_{10}). This was not observed in cigarette smoke and fuel exhaust. Both particle types showed much lower C_n chains. Soot and biomass burning can be

separated by the presence of K^+ (m/z 39). Engine exhaust particle showed a peak at m/z 40 (most likely calcium, as also reported by Shields et al. (2007) and Trimborn et al. (2002). Cigarette smoke particles show the markers similar to PAH particles (m/z 50, 51, 63, 77), but additionally the C_n chain which is not contained in the PAH reference spectra.

A particle type "cigarette smoke" was not found at the Jungfraujoch, but the types PAH and soot. Both were merged to one particle type in Figure 3.

Changes to text:

The particle types that were assigned to the type "engine exhaust" also show C_n-fragmentation ($C_1^+ – C_5^+$, m/z 12 … 60) but can be distinguished by the peak at m/z 40 (Ca^+) which was observed in the reference mass spectra but also previously by other researchers (Trimborn et al., 2002; Vogt et al., 2003; Shields et al., 2007).

PAH containing particle were identified through the corresponding reference spectra and marker peaks from the laboratory studies, namely 50/51 ($C_4H_2/_3^+$), 63 ($C_5H_3^+$), 77 ($C_6H_5^+$), and 91 ($C_7H_7^+$). Even though cigarette particles (before inhalation) contain these markers as well, our reference spectra indicate that these two particle types can be distinguished because cigarette smoke additionally contains a C_n pattern (m/z 12 – 36).

5d- Please add proposed/suggested elemental formulas to each ion in Table 3. Currently only Cn peaks are identified.

This is a good suggestion. We added the elemental formulas to the table (now Table 2).

5e- p8,1-3 discusses that "biological particles" showed marker peaks related to aminelike or oxidized organic structures. How have these particles been identified as biological and not simply amine-like? If the particle type cannot be unambiguously identified as biological, it should be called "biological/amine" or similar, as was done for sea salt/cooking. I don't see how these particles were recognized as biological.

We found two particle types that we assigned to biological particles (Figure 2):

Type 1 shows peaks at m/z 18, 30, 39, 58, and 59.

Type 2 shows peaks at m/z 23, 27, 40, 47.

The marker peaks found from the reference spectra (Table 2) show that ground maple leaves show exact the marker peaks 18, 30, 39, 58, while pollen show 39, 58, 59. This is the reason to assign "type 1" to biological particles. We used "amine-like" to explain the occurrence of m/z 59, which may be $(CH_3)_3N^+$, a marker for trimethylamine (e.g., Healy et al., 2014). Also m/z 18, 30, and 58 can be explained by nitrogen-containing ions (NH_4^+, CH_4N^+, and $C_3H_8N^+$). The identification of "type 2" as biological relies mainly on m/z 47 (PO_3^+), observed in pollen and in bacteria.

We changed the name of this particle type in Figures 3, 4 and 7 to "biological/amine".

5f- The ambiguity between sea salt and cooking emissions is a significant issue. Were there no complementary measurements, eg AMS or molecular markers, performed during this field study which could help to udnerstand the nature of these particles? Moreover, I don't understand why there is any ambiguity since I can see more than one unique peak for sea salt in Table 3. e.g. 135 and 158. Or could peak heights be used?

It is explained in the manuscript (page 4 lines 1-2) that only cations were available from the Jungfraujoch field data. Thus, the anion marker peaks at 135 and 158 could not be used. The cation markers (23, 46, 81, 83, 139) occur both in sea salt and in cooking emissions (most likely from salt contained in the spicing of the meat), so from cations alone these two particle types can't be distinguished, as was explained on page 8 in lines 7-9.

There are reasons to believe that these particle are more likely from cooking that from sea salt, because Fröhlich et al. (2015) report from Jungfraujoch the observation of local POA that resembles organic aerosol from cooking (COA), but our data base (we only observed 39 particles of this type in the IPR population and none in the out-of-cloud aerosol) is too small to draw further conclusions.

5g- how has the PAH cluster been identified? I do not see any PAHs listed in the laboratory samples and I missed a discussion in the text. It looks like some aromatic related peaks are present but are they polyaromatic?

Both Table 1 and Table 2 of our manuscript list PAH. We used benzo[ghi]perylene, dibenzo(a,h)anthracene and triphenylene. We will specify this in Table 1. Table 2 and the mass spectra now added to the supplement show that the marker peaks like 50, 51, 63, 77, 91 are well suited to identify this particle type. Cigarette smoke (before inhalation) shows these markers as well, but that's not surprising because cigarette smoke contains PAHs. However, we did not study other aromatics up to now.

5h- Since reference spectra of pure composition were used, the manuscript should discuss the possibility of matrix effects when internally mixed atmospheric particles were measured.

We added a discussion on this important point (section 3.1). It is also desirable to investigate these matrix effects with mixture of the reference particle types presented here, but this has to be a subject of future work.

It has to be noted that matrix effects may complicate the identification of particle types by markers peaks. Here we have only analyzed pure substances (with exception of the source sampling types and the natural dust samples). But in laser ablation mass spectrometry, the ionization efficiency can be a function of the particle matrix (e.g., Gross et al., 2000) such that marker peaks of certain particle types might be less abundant in internal particle mixtures. Future studies will therefore also include reference mass spectra from various types of mixed particles.

6-
p6,20 What is the probability of a small particle passing through the CVI? I can imagine

that the ratio N(ice) / N(total) is similar to the ratio prob(small) / prob(large), so that small particle leakage could be a significant source of error.

Although we do not really agree that the ratio N(ice) / N(total) is similar to the ratio prob(small) / prob(large), we are aware that there might be a chance that particles below the CVI cut-size might overcome the counterflow. This was shown for the rather new concept of a pumped CVI (PCVI) by Pekour and Cziczo (2011). According to their work, the transmission of small particles should be caused by collisions, coagulation or riding the wake of particles with diameters larger than the CVI lower cut-off size, but could also be due to the different design, which creates flow imperfections in contrast to the "classical" CVI. Up to now this issue of small particle leakage was never investigated but also never observed for the CVI design used in this study. Nevertheless, we applied the simulation results for the PCVI to estimate the contribution of small particle leakage. Pekour and Cziczo (2011) provide values for the ratio $n_{out}/(n_{in} \times N_{out})$ for different sizes and as a function of the PCVI counterflow, where n_{out}, n_{in}, and N_{out} denote the concentration of small transmitted (smaller than the CVI cut-off size), small initial, and large transmitted (larger than the CVI cut-off size) particles. Their results show that for the used counterflows this ratio is on the order of 10^{-5} cm^{-3}. So, the ratio of leaked small particles (n_{out}) to correctly sampled large particles (N_{out}) is

$$n_{out}/N_{out} = 10^{-5}\ cm^{-3} \times n_{in}.$$

This means that only for high background aerosol number concentrations ($10^3 - 10^4$ cm^{-3}), the fraction of small leaked particles could be 1 – 10 % of the correctly sampled residual particles, but most of the time it should be below 1 % at the conditions at the Jungfraujoch where particle concentrations in winter and spring are typically below 1000 cm^{-3} (Herrmann et al., 2015).

7-
p11,9-14 I am not convinced by the argument that Kdominated particles were biomass burning simply because they were smaller, although it is an interesting hypothesis. Perhaps the authors could use their laboratory data to investigate this hypothesis.

We agree, this conclusion is not valid. The size distribution of the K-dominated (Fig. 4) particles looks different than that of biological and biomass burning particles. Thus, it is unlikely that the source of these K-dominated particles is biological or biomass burning. We modified the text accordingly:

The out-of-cloud aerosol shows an increased number fraction of biological particles between 200 and 400 nm and larger than 1000 nm. The number of potassium-dominated particles is decreasing with particle size while the highest number of biomass burning particles is found in the size range from 300 nm up to 1000 nm. Thus, it is unlikely that the potassium-dominated particles originate mainly from biological particles or from biomass burning.

8-
The larger average size of IPR is interpreted as indicative that larger particles are better INP. Has the alternative hypothesis that larger particles pass more easily through the sampling apparatus and CVI been excluded?

The transmission of the ALABAMA and the OPC themselves would cancel out, but the sampling line transmissions might play a role, because the sampling line from the CVI was shorter (126 cm) than that from the total inlet (261 cm). We calculated the transmission (as already stated in the manuscript), and divided the transmission curves. The ratio $transmission_{CVI}$ to $transmission_{total}$ does not deviate significantly from unity between 100 nm (ratio = 1.005) and 1500 nm (ratio = 1.04). Thus, we can rule out that sampling losses are an issue here.

9-
p12,15-21. Here the authors argue that relatively more PAH/soot particles were measured during one episode because the air mass rose higher and preferentially lost other better CCN particles to wet removal. Comparing absolute instead of relative numbers would better test this hypothesis. The speculation of picking up additional local emissions after rising higher is not justified since the air mass did not fall especially low after rising higher. Either a complete and detailed analysis is needed to test this hypothesis, or the speculation should be omitted.

We agree with the reviewer that this assumption is too speculative and we skip this suggestion, because a detailed analysis of the air mass history would be beyond the scope of this paper.

10-
on p12,8, "these findings agree with the general statement that natural primary aerosol such as biological particles, soil dust or minerals serve as typical ice nucleators" does not come across as a scientific. Why is this general statement being proposed? If because of recent publications, then the citations are missing. If I am not mistaken, what the current manuscript provides is a valuable demonstration of the presence of such IPR in the field (if the statistical analysis indicates that these conclusions are robust and if proper consideration to amine or other interpretations of "biological" are given). A better phrasing of this statement would be something like, "This case study illustrates the potentially significant contribution of biological, soil dust, minerals, and sea salt/cooking emissions on INP concentrations in mixed phase clouds, as has been identified in the laboratory (citations)".

This is a misunderstanding. This section discusses the case study where we compared IPR and out-of-cloud aerosol for two time periods with very similar air mass origin and meteorological conditions. This sentence was meant to compare the case study (Fig 7) with the whole data set (Fig 3). We have rephrased the sentence:

This case study shows that the observed differences between IPR and out-of-cloud aerosol particles that were observed when looking at the whole data set (Fig 3) cannot be explained by differences in meteorological conditions and air mass origin. The finding that natural primary aerosol particles such as biological particles, soil dust and minerals are enhanced in the IPR population is valid for both data sets.

11-
The only category for organic aerosol in this study was "aged material" which contributed 30% of the total out of cloud particle number.
It is my opinion that the chemical composition measured by ALABAMA is highly skewed relative to the chemical composition measured by quantitative techniques (e.g. AMS OA,

sulfate, nitrate, and ammonium, combined with dust and EC). Presumably the ALABAMA instrument therefore has significant biases towards or against certain species. A detailed and quantitative discussion of instrument sensitivity towards different species must be included in this manuscript, if the reported pie charts are to be interpreted quantitatively.

It has to be understood that particle type and mass concentration are two completely different ways of looking at aerosol particle population. For example, consider a uniform monodisperse particle population, where each particle contains 30% NH_4NO_3, 30% $(NH_4)_2SO_4$, and 40% organic matter, the ALABAMA (ATOFMS, PALMS, SPLAT, LAAPTOF, LAMPAS…)-technique can only yield one particle type, while AMS will report the 4 quantities. Both of them are correct, though.

Organic aerosol reported from AMS measurement is frequently further resolved by PMF analysis, and the resulting factors are typically HOA, COA, BBOA, OOA (sometimes divided into LV-OOA and SV-OOA). In the ALABAMA data we detected similar particle types: engine exhaust (similar to HOA), biomass burning particles (BBOA), and even cooking emissions (although we have the interference with sea salt in this special case). The OOA (oxygenated organic aerosol) component is typically interpreted as aged organic aerosol by the AMS user community (to which we also belong). Thus, OOA-dominated particles will fall into the "aged material" type in the single particle analysis. As no anions were available during the Jungfraujoch measurements, nitrate and sulfate could not directly be detected. NH_4^+ (m/z 18), however, is an indicator for ammonium nitrate or ammonium sulfate. The particle assigned to the particle type "aged material" contain both the organic marked fragments and the NH4 markers, such that we assume internal mixture of secondary inorganic and organic particles.

We also have to note here that single particle laser ablation mass spectrometry is not a new technique. There have been numerous publications since about 1998 that use automatic clustering algorithms and marker peak search for the assignment of particle spectra to certain particle types and report the results as pie charts (or other form of graphic visualization). We therefore think that a detailed and quantitative discussion of instrument sensitivity towards different species is beyond the scope of this manuscript. We use the same ablation laser at the ATOFMS instrument or the SPASS instrument (a 266 nm Nd:YAG), so we can refer the reader to earlier publications of the Prather group (e.g. Pratt and Prather, 2010; Pratt et al., 2009; .), other ATOFMS users (e.g., Sierau et al., 2014; Kamphus et al., 2010), and SPASS users (Erdmann et al., 2005; Hinz et al., 2006).

We added a short paragraph to section 2.2:

Typically, the assignment of mass spectra to a certain particle type relies on the most abundant marker peaks. Therefore, smaller species that are abundant on many or even all particle types might go unnoticed. Thus is most likely the case for secondary inorganics (sulfate, nitrate) and secondary, oxygenated organics, which may add a coating to mineral dust particles, but the particle signal is still dominated by the mineral dust signatures. Thus it has to be kept in mind that a particle type called "mineral" should be read as "mineral-dominated". The only exception we made here is the particle type "lead-containing" where we explicitly state that lead does not represent the whole particle composition. Such a classification of particles is very common in the single particle mass spectrometry literature. The ALABAMA uses a 266 nm ND:YAG laser for particle ablation and ionization, thus we expect the assignment of mass

spectra to be similar to other instruments using the same laser wavelength (ATOFMS, SPASS) of which many results on the abundance of particle types similar to our classification have been reported (Pastor et al., 2003; Erdmann et al., 2005; Hinz et al., 2006; Pratt et al., 2009; Kamphus et al., 2010; Pratt and Prather, 2010; Sierau et al., 2014).

12-
As the authors note, the present data do not allow ice nucleation rates for different particle types to be determined. Therefore please change "particles have good ice nucleating ability" to "particles were observed within ice crystal residuals" on p12,26 and please change "The high ice nucleation ability of etc etc could be confirmed" to "The presence of INP from etc etc was observed". This avoids overstating the results, which are nonetheless valuable and interesting.
The authors may also improve their manuscript by comparing the relative fractions of each particle type they have observed to previous studies of IPR or IN composition. That is, by comparing to the Cziczo citation given later in this review and the various citations already present in the manuscript. Although ice nucleation rates cannot be determined, a quantitative comparison in another dimension can nevertheless be added.

We changed the text as suggested.

We included a more detailed comparison of our observed particle type in IPR with those reported by Kamphus et al from the same site and also by Cziczo et al., 2013. However, it has to emphasized that Cziczo 2103 discussed cirrus clouds, where the formation processes, especially temperatures, are very different to mixed phase clouds.

Added text:

The general trend of this finding agrees with the only result so far in the literature on single particle mass spectrometric analysis of IPR from mixed phase clouds (Kamphus et al., 2010): Using two single particle mass spectrometers, they report from one instrument (SPLAT) that 57% of all IPR were mineral particles or mixtures of minerals with sulfate, organics, and nitrate. The other instrument (ATOFMS) reported that these two particles types represent a much higher fraction (78%) of all IPR, plus additionally 8% metallic particles. However, these data sets are based on smaller numbers of particle than our study (ATOFMS 152 particles, SPLAT 355 particles), such that here variations of air mass origin and meteorological conditions can be the main reason for such differences and none of these data sets can be regarded as representative for mixed phase clouds at the Jungfraujoch in general. A recent paper by Cziczo et al. (2013) summarized their analyses of ice crystals on various field studies. Although formation of cirrus clouds occurs under different conditions that ice formation in mixed phases clouds, it is interesting to compare these results as well. These data clearly show that mineral dust is the most dominant heterogeneous ice nucleus in all cirrus encounters, but that under homogeneous freezing conditions the upper tropospheric background aerosol particles (sulfate/organic/nitrate) as well as biomass burning particles are detected in the cirrus IPR.

Minor:

- Percentages of particle types are frequently reported, but it is not always clear what the reference is (% of all IPR vs % relative to all of that particle type?). Please give a universal definition in Section 2. Please also add uncertainties to each reported %.

We added the definition of the percentage to section 2

"We report the absolute number of particles of the particle type in a certain time period and the percentage of these particles to the total particle population (i.e, the sum of all particle types) measured during the same time period."

We added uncertainties (as explained above) to all values.

Section 3.2.1. Some particle types are given no discussion at all (engine and PAH) while others are given extensive discussion (industrial and lead). If there is some reason why engine and PAH particles were not further discussed, please make a brief note for the reader.

As already mentioned above, we added a discussion on engine exhaust particles and PAH-containing particles on in section 3.2.1:

The particle types that were assigned to the type "engine exhaust" also show C_n-fragmentation ($C_1^+ – C_5^+$, m/z 12 … 60) but can be distinguished by the peak at m/z 40 (Ca^+) which was observed in the reference mass spectra but also previously by other researchers (Trimborn et al., 2002; Vogt et al., 2003; Shields et al., 2007).

PAH containing particle were identified through the corresponding reference spectra and marker peaks from the laboratory studies, namely 50/51 ($C_4H_2/_3^+$), 63 ($C_5H_3^+$), 77 ($C_6H_5^+$), and 91 ($C_7H_7^+$). Even though cigarette particles (before inhalation) contain these markers as well, our reference spectra indicate that these two particle types can be distinguished because cigarette smoke additionally contains a C_n pattern (m/z 12 – 36).

- p3,21 This description of LDI (laser desorption/ionization) incorrectly implies two-step vaporization and ionization. The laser does not "vaporize a fraction of created gas molecules" since ionization can occur during desorption. Better would be "the pulsed laser fires and vaporizes/ionizes the particle partly or completely."

Agreed. We changed the text accordingly.

- p3,25 what refractive index was assumed for particle sizing?

The Grimm 1.129 is calibrated with PSL particles, refractive index = 1.60. We added this information in section 2.1.

- p4,33 cooking is not combustion, so change "directly produced by combustion" to "directly sampled from the source"

Changed.

- p4,33 I believe "supernatant" is the scientific term for "washing water"

Agreed, we used the scientific term but kept "washing water" in parentheses since it was used in previous publications (Augustin et al., 2013; Augustin-Bauditz et al., 2016).

p5,3 when using the word majority, please give a number

The number of spectra representing the majority differs between particle types. The supplement now shows the spectra from the laboratory measurement. It was found that one reference particle type produced several types of spectra which were separated using the clustering algorithm described above. The supplement lists the main clusters with the number of spectra in each cluster.

p5,29 does the manual switching mean that there is some bias in the results? Was there always a cloud free period measured at the end of the in cloud periods? Please clarify.

"Manual switching" means that no automated valve was used that would be controlled by a cloud droplet sensor. When a cloud was present, we sampled though the ice-CVI, when no cloud was present, we sampled through the aerosol inlet. Sampling though the CVI under non-cloud condition corresponds to a zero measurements because no particles enter the CVI.

We changed the text to: "Under cloud conditions the ALABAMA sampled through the Ice-CVI, whereas under cloud-free condition it was switched manually to the total aerosol inlet."

p6,14, what is meant by "ambient temperatures below 0 C"? Either ambient, or below 0 C.

We rephrased this sentence to make it more clear:

The impaction plates of the pre-impactor are not actively cooled but adopt ambient temperature which must be below 0°C to allow for mixed phase clouds to exist.

p7,18 please define "PAH fragmentation" including citations. Can "PAH" be recognized separately from "aromatic"?

The fragmentation pattern of PAHs was measured during our laboratory studies. We included the mass spectra in the supplement.
We rephrased the sentence: "The particles from smoke after inhalation do not show the characteristic marker peaks that were observed for PAH particles in the laboratory study."

Unfortunately no other aromatics were measured in the laboratory, thus we cannot make a statement on this issue.

p7,20 please give the physical reason why only sodium or potassium would be observed.

This is due to the non-uniform laser ablation and ionization process. Sodium and potassium are present in pollen and biomass burning particles. Apparently (as the laboratory data show) it occurs that only these two ions are produced upon laser ablation/ionization.

We reformulated the sentence:

"It was observed that some rare fragmentation patterns from pollen and biomass burning particles show similarities within the cation spectra (only one sodium (m/z 23) and potassium (m/z 39) peak). This is most likely due to the non-uniform laser ablation and ionization process, leading to production of only those two ions."

p9,30 please cite a paper for this point

This statement was a tentative explanation of the finding that sometimes only a single potassium peak is observed in the cation mass spectrum. While there are references confirming that laser ablation is very sensitive to potassium (Gross et al., 2000; Silva and Prather, 2000), we can't find a reference for the speculation that other ions are suppressed. Thus, we rephrased the sentence:

It must be taken into account that the detection of potassium in laser ablation mass spectrometry is very efficient due to its low ionization efficiency (Gross et al., 2000; Silver and Prather, 2000), such that only a small amount of potassium in a particle results in a large ion signal.

p9,34 I don't understand the motivation behind this sentence. The message seems to be that a similar number fraction of biomass burning particles in the aerosol and in the IPR is an unexpected result. Why would it be unexpected?

We reformulated the whole paragraph, as it was indeed hard to understand. It reads now:

The IPR ensemble contains particles assigned to engine exhaust but no particles assigned to biomass burning. This finding is surprising because both particle types have been detected in IPR before: biomass burning by Kamphus et al. (2010), Twohy et al. (2010), Pratt et al. (2011) and Prenni et al. (2012), and engine exhaust by Kamphus et al. (2010) and Corbin et al. (2012). Both engine exhaust and biomass burning particle contain organic material and the mass spectra show partly similar peaks, thus it is unclear which specific property of these particle types enables their ice nucleation ability. The third particle type associated with combustion (PAH/soot) is found in both populations in the same percentage (12%). The source of these particles can also be biomass burning or engine exhaust (as well as other combustion processes), but the finding that the percentage in both populations is equal suggests that the PAH/soot components are not significantly influencing the ice nucleation capability.

Fig 2 and 6. Please add uncertainties for all values. Please sort the table by either out-of-cloud or IPR values. Please add a column to the table "%IPR / %out-of-cloud" to estimate the relevance enhancement of each category, including uncertainties.

We added the uncertainties that were estimated as explained above, and also added the suggested column giving the enhancement. However, we prefer to keep both pie charts and the table in the order as it is now. The particle types are ordered from biological/natural to anthropogenic/industrial, followed by the unassigned, descriptive types "K dominated" and "Na + F" and "others".

-The following articles should be cited in this manuscript: Jaenicke, Abundance of Cellular Material and Proteins in the Atmosphere, Science, 308, 5718, pp 73, 2005. Cziczo et al., Clarifying the Dominant Sources and Mechanisms of Cirrus Cloud Formation, Science, 340, 6138, pp 1320-1324.

We included citations to these articles.

Very minor comments:

p1,20, unclear wording. try, "the outcome of these laboratory studies was particle type specific marker peaks for each investigated particle type."

Changed to: "The outcome of these laboratory studies was characteristic marker peaks for each investigated particle type. These marker peaks were applied to the field data."

p2,5 starting from "therefore" is a repetition of the previous statement which takes some thinking to realize.

We deleted the second part of the sentence.

p2,22 please also discuss Cziczo et al., Science 2013.

We have included a reference to Cziczo et al., 2013.

p2,28 "first results" to me is synonymous with "preliminary results". Perhaps better is "Inspection of the data set showed"

Changed

p10,35-37. "does not represent the real distribution" is more clearly phrased as "is not corrected for sampling and detection efficiency"

Changed to:

"It must be emphasized here that the ALABAMA size distribution is not corrected for sampling and detection efficiency, the latter being optimal around 400 nm."

p11,27 with temperature and relative humidity, the wet-bulb temperature is already given?

Yes, but not straightforward (Stull, 2011), thus we preferred to look at the wet-bulb temperature directly as it was supplied by MeteoSwiss.

References

Augustin, S., Wex, H., Niedermeier, D., Pummer, B., Grothe, H., Hartmann, S., Tomsche, L., Clauss, T., Voigtländer, J., Ignatius, K., and Stratmann, F.: Immersion freezing of birch pollen washing water, Atmos. Chem. Phys., 13, 10989-11003, doi:10.5194/acp-13-10989-2013, 2013.

Augustin-Bauditz, S., Wex, H., Denjean, C., Hartmann, S., Schneider, J., Schmidt, S., Ebert, M., and Stratmann, F.: Laboratory-generated mixtures of mineral dust particles with biological substances: characterization of the particle mixing state and immersion freezing behavior, Atmos. Chem. Phys., 16, 5531-5543, doi:10.5194/acp-16-5531-2016, 2016.

Bezdek, J. C., Ehrlich, R., and Full, W.: FCM: The fuzzy c-means clustering algorithm, Computers & Geosciences, 10, 191-203, 1984.

Corbin, J. C., Rehbein, P. J. G., Evans, G. J., and Abbatt, J. P. D.: Combustion particles as ice nuclei in an urban environment: Evidence from single-particle mass spectrometry, Atmospheric Environment, 51, 286-292, 2012.

Cziczo, D. J., Froyd, K. D., Hoose, C., Jensen, E. J., Diao, M., Zondlo, M. A., Smith, J. B., Twohy, C. H., and Murphy, D. M.: Clarifying the Dominant Sources and Mechanisms of Cirrus Cloud Formation, Science, 340, 1320-1324, doi: 10.1126/science.1234145, 2013.

Erdmann, N., Dell'Acqua, A., Cavalli, P., Gruning, C., Omenetto, N., Putaud, J. P., Raes, F., and Van Dingenen, R.: Instrument characterization and first application of the single particle analysis and sizing system (SPASS) for atmospheric aerosols, Aerosol Science and Technology, 39, 377-393, doi: 10.1080/027868290935696, 2005.

Fröhlich, R., Cubison, M. J., Slowik, J. G., Bukowiecki, N., Canonaco, F., Croteau, P. L., Gysel, M., Henne, S., Herrmann, E., Jayne, J. T., Steinbacher, M., Worsnop, D. R., Baltensperger, U., and Prévôt, A. S. H.: Fourteen months of on-line measurements of the non-refractory submicron aerosol at the Jungfraujoch (3580 m a.s.l.) – chemical composition, origins and organic aerosol sources, Atmos. Chem. Phys., 15, 11373-11398, doi: 10.5194/acp-15-11373-2015, 2015.

Gross, D. S., Gälli, M. E., Silva, P. J., and Prather, K. A.: Relative Sensitivity Factors for Alkali Metal and Ammonium Cations in Single-Particle Aerosol Time-of-Flight Mass Spectra, Analytical Chemistry, 72, 416-422, doi: 10.1021/ac990434g, 2000.

Herrmann, E., Weingartner, E., Henne, S., Vuilleumier, L., Bukowiecki, N., Steinbacher, M., Conen, F., Collaud Coen, M., Hammer, E., Jurányi, Z., Baltensperger, U., and Gysel, M.: Analysis of long-term aerosol size distribution data from Jungfraujoch with emphasis on free tropospheric conditions, cloud influence, and air mass transport, Journal of Geophysical Research: Atmospheres, 120, 9459-9480, doi: 10.1002/2015JD023660, 2015.

Hinz, K.-P., Greweling, M., Drews, F., and Spengler, B.: Data Processing in On-line Laser Mass Spectrometry of Inorganic, Organic, or Biological Airborne Particles, American Society for Mass Spectrometry, 10, 648-660, 1999.

Hinz, K. P., Erdmann, N., Gruning, C., and Spengler, B.: Comparative parallel characterization of particle populations with two mass spectrometric systems LAMPAS 2 and SPASS, International Journal of Mass Spectrometry, 258, 151-166, doi: 10.1016/j.ijms.2006.09.008, 2006.

Kamphus, M., Ettner-Mahl, M., Klimach, T., Drewnick, F., Keller, L., Cziczo, D. J., Mertes, S., Borrmann, S., and Curtius, J.: Chemical composition of ambient aerosol, ice residues and cloud droplet residues in mixed-phase clouds: single particle analysis during the Cloud and Aerosol Characterization Experiment (CLACE 6), Atmospheric Chemistry and Physics, 10, 8077-8095, 2010.

Pastor, S. H., Allen, J. O., Hughes, L. S., Bhave, P., Cass, G. R., and Prather, K. A.: Ambient single particle analysis in Riverside, California by aerosol time-of-flight mass spectrometry during the SCOS97-NARSTO, Atmospheric Environment, 37, S239-S258, doi: 10.1016/s1352-2310(03)00393-5, 2003.

Pekour, M. S., and Cziczo, D. J.: Wake Capture, Particle Breakup, and Other Artifacts Associated with Counterflow Virtual Impaction, Aerosol Science and Technology, 45, 758-764, doi: 10.1080/02786826.2011.558942, 2011.

Pratt, K. A., Mayer, J. E., Holecek, J. C., Moffet, R. C., Sanchez, R. O., Rebotier, T. P., Furutani, H., Gonin, M., Fuhrer, K., Su, Y. X., Guazzotti, S., and Prather, K. A.: Development and Characterization of an Aircraft Aerosol Time-of-Flight Mass Spectrometer, Analytical Chemistry, 81, 1792-1800, doi: 10.1021/ac801942r, 2009.

Pratt, K. A., and Prather, K. A.: Aircraft measurements of vertical profiles of aerosol mixing states, Journal of Geophysical Research-Atmospheres, 115, D11305, 2010.
Pratt, K. A., Murphy, S. M., Subramanian, R., DeMott, P. J., Kok, G. L., Campos, T., Rogers, D. C., Prenni, A. J., Heymsfield, A. J., Seinfeld, J. H., and Prather, K. A.: Flight-based chemical characterization of biomass burning aerosols within two prescribed burn smoke plumes, Atmospheric Chemistry and Physics, 11, 12549-12565, 2011.
Prenni, A. J., DeMott, P. J., Sullivan, A. P., Sullivan, R. C., Kreidenweis, S. M., and Rogers, D. C.: Biomass burning as a potential source for atmospheric ice nuclei: Western wildfires and prescribed burns, Geophysical Research Letters, 39, L11805, 2012.
Roth, A.: Untersuchungen von Aerosolpartikeln und Wolkenresidualpartikeln mittels Einzelpartikel-Massenspektrometrie und optischen Methoden, PhD thesis, University of Mainz, Germany, urn:nbn:de:hebis:77-37770, 2014.
Roth, A., Schneider, J., Klimach, T., Mertes, S., van Pinxteren, D., Herrmann, H., and Borrmann, S.: Aerosol properties, source identification, and cloud processing in orographic clouds measured by single particle mass spectrometry on a Central European mountain site during HCCT-2010, Atmospheric Chemistry and Physics 15, 24419-24472, 2016.
Shields, L. G., Suess, D. T., and Prather, K. A.: Determination of single particle mass spectral signatures from heavy-duty diesel vehicle emissions for PM2.5 source apportionment, Atmospheric Environment, 41, 3841-3852, doi: 10.1016/j.atmosenv.2007.01.025, 2007.
Sierau, B., Chang, R. Y. W., Leck, C., Paatero, J., and Lohmann, U.: Single-particle characterization of the high-Arctic summertime aerosol, Atmos. Chem. Phys., 14, 7409-7430, doi: 10.5194/acp-14-7409-2014, 2014.
Silva, P. J., and Prather, K. A.: Interpretation of Mass Spectra from Organic Compounds in Aerosol Time-of-Flight Mass Spectrometry, Analytical Chemistry, 72, 3553-3562, doi: 10.1021/ac9910132, 2000.
Stull, R.: Wet-Bulb Temperature from Relative Humidity and Air Temperature, Journal of Applied Meteorology and Climatology, 50, 2267-2269, doi: doi:10.1175/JAMC-D-11-0143.1, 2011.
Trimborn, A., Hinz, K. P., and Spengler, B.: Online analysis of atmospheric particles with a transportable laser mass spectrometer during LACE 98, Journal of Geophysical Research: Atmospheres, 107, LAC 13-11-LAC 13-10, doi: 10.1029/2001JD000590, 2002.
Twohy, C. H., DeMott, P. J., Pratt, K. A., Subramanian, R., Kok, G. L., Murphy, S. M., Lersch, T., Heymsfield, A. J., Wang, Z., Prather, K. A., and Seinfeld, J. H.: Relationships of Biomass-Burning Aerosols to Ice in Orographic Wave Clouds, Journal of the Atmospheric Sciences, 67, 2437-2450, 2010.
von der Weiden, S. L., Drewnick, F., and Borrmann, S.: Particle Loss Calculator – a new software tool for the assessment of the performance of aerosol inlet systems, Atmos. Meas. Tech., 2, 479-494, 10.5194/amt-2-479-2009, 2009.

Reply to the follow-up comment by reviewer #1

Initial comment from the reviewer:
3- In Section 2.3 when discussing the lab spectra it is stated "only those mass spectra that represented the majority of the different fragmentation patterns were considered".
What % defines majority? Moreover, this % should be used to define a correction factor (with corresponding uncertainty propagated into the result). If only 60% of particles were measured for salt but 90% for soot, then the reported IPR numbers should be scaled up by 1/0.6 and 1/0.9 respectively.

> Response by the authors:
>
> Correction of the reported IPR numbers can't be done in this way. First, we might end up with more particles that were actually measured. Second, it is only possible to assign marker ions of atmospheric particles to those reference spectra containing these marker ions. Speculating about spectra not containing the markers would only increase the uncertainty.

"follow-up comment" from the reviewer:
I'm not quite convinced by the arguments in this response. It would be appropriate to end up with more particles than were measured, if a correction for missed particles was applied. There are 2 ways the ALABAMA may miss particles. The obvious way is if the instrument only obtains a signal for, say, 10% of all particles (90% "missed"). Then a correction factor 1/0.1 should be applied. The second way is if the instrument obtains a full mass spectra (with marker ions) for 10 of 100 biomass burning particles and only a partial mass spectra (eg no signals except potassium) for 30 of 100 biomass burning particles. We can suppose that their remaining 60 are missed particles. In the second case, the correct number to be reported for the biomass burning class is 10*1/0.1.
There is ambiguity about what to do with the 30 partial mass spectra: they could be put into a category "other" but careful thought would be needed before reporting total estimates for number concentration.
It is essential to include such a correction factor if the goal is to compare the abundances of different particle types. If a correction factor is not applied, it must be proven that the conclusions are unchanged by its omission – it is only valid to omit the correction if it would be similar for all particle types, in analogy to weighting or not weighting a linear regression. Therefore I still think that the manuscript should include a report (discussion/table/graph) of the fraction of laboratory samples which included the marker ions and which did not. If this fraction was very different between classes, the comparative statistics in the abstract (13% dust, 3% aged particles in IPR) would be incorrect. There is another subtlety which I would like to state but do not expect the authors to address. A biomass burning particle missing certain markers may possibly be classified as aged, which would mean a second-order correction of overlapping particle classes could be made (this is just an example, and not based on the authors' marker ions). Without this correction, particle type numbers could indeed be overestimated, but I imagine this would be pushing the data analysis past what is reasonable.

> Reply by Johannes Schneider (on behalf of all co-authors):
>
> We considered the follow-up comment very carefully, but we still think that such a correction is not possible. We list our arguments here:
>
> 1. "missed particles": It would be necessary to determine a size-resolved detection efficiency for all reference particles. We did not size-select the test particles, but parallel measurements with an optical particle sizer are available. However, some uncertainty

would result from this, because of the necessary conversion of the different equivalent diameters.

2. Assuming such size-dependent correction factors are available, a major obstacle is that parameters inferred from pure, laboratory-generated particles or directly form the source sampled particles can not be transferred to aged, processed particles found in the ambient atmosphere. The shape of freshly emitted soot or combustion particles will change through atmospheric processing from very non-spherical to more spherical, thereby improving the focusing properties of the particles in the aerodynamic lens. Thus, the detection efficiency will improve by processing. Also, non-spherical dust particles can be coated by secondary organic or inorganic material, leading to a more spherical shape. Matrix effects, altering the ionizations process of internally mixed particles compared to the pure laboratory particles are also possible.
3. Particles that are ionized but do not show the marker peak spectra: Here the same argument as above holds: We would compare the pure laboratory particles to aged and processed atmospheric particles.
4. Particles that are ionized but that do not show the marker peaks would in the current analysis either assigned erroneously to another particle type or to the group "others". Since it is not known where these falsely assigned particle end up, we can't correct for this error, too. Please note also that the cluster "others" is by far not large enough to account for all possible particle not showing the marker peaks. Additionally, although we investigated a large number of reference particles, there will by a large number of possible atmospheric particle types that we did not investigate and which may be included in the "others" group. Thus, subtracting particle from the "others" cluster is not a valid option.

Summarizing, we think that trying to correct for all these effects would lead to unacceptably high uncertainties and should not be done, neither for ALABAMA nor for any other single particle mass spectrometer, and has to our knowledge not been done by other groups.

In contrast, we prefer to understand the relative abundances and absolute numbers of particles as "number of particles identified by the ALABAMA" and not as "number of particles in the ambient atmosphere". We will clarify this in the text and in the figure captions. We will also add a discussion of the points above to the manuscript.

Nevertheless, comparison between the out-of-cloud aerosol and the ice residuals (which is the focus if this manuscript) is possible, because, to the best of our knowledge, the above effects affect both particle populations in the same way.

We added the following text to section 2.3:

It should be further kept in mind that the detection and ablation/ionization efficiency of the ALABAMA (and of most other single particle instruments) is not equal for all particle types. Additionally, the observation that only a fraction of each reference particle type showed the characteristic marker peaks leads to a further bias of the data. It therefore has to be emphasized that the reported particle numbers and relative abundances refer only to particles detected by the ALABAMA and not to their real abundance in the atmosphere. However, comparison

between different particle populations is meaningful, because the same biases hold for all sampling periods.

acp-2016-365

Schmidt et al., On-line single particle analysis of ice particle residuals from mountain-top mixed-phase clouds using laboratory derived particle type assignment

Reply to Reviewer #2

Reviewer comments and questions are printed in this font type.

Our replies are printed like this.

Changes to the manuscript text are printed in blue.

The manuscript by Schmidt et al. presents ambient and laboratory single particle mass spectrometer data to identify chemical components in aerosols and ice residuals on Jungfraujoch and to draw conclusions on the ice nucleation ability of different aerosol particle components. Given the importance of ice nucleation processes for precipitation and the climate, and the many uncertainties related to these processes, such studies are needed. The combination of laboratory experiments and ambient measurements makes this study especially useful for the single particle mass spectrometer community. I therefore recommend publication of this well-written manuscript in ACP after the following comments have been addressed:

We thank the reviewer for the positive rating of our manuscript

General comments

The limitations and uncertainties of single particle mass spectrometry and the respective data should be addressed in more detail.

There are several aspects:
- More care should be given as how one describes the quantities. It should be made clear, e. g. in the introduction, that “a larger relative amount” cannot be interpreted as “more aerosol mass”, but can only refer to “a larger number of particles” assigned to a certain category.

Agreed. This is a very important point for laser ablation single mass spectrometry. We replaced "relative amount" by "number fraction" in the abstract, in section 3.2.2 and 3.2.4, and in the summary.

- The presentation of marker mass fragments and reference spectra from different particle types is highly desirable for the single particle mass spectrometer community. For the spectra to be useful for other groups/instrument types however, information on uncertainties needs to be given. One of the issues of laser ablation single particle mass spectrometers is the (weak) repeatability of spectra/measurements; depending on particle size, chemical composition/morphology, and on the placement of the particle in the laser beam, the amount of ablated/ionized material can vary significantly. According to p. 4, l. 36, you were not size-selecting particles for your laboratory tests, which might have led to larger spectrum-to-spectrum differences. Showing e. g. standard deviations of the averaged spectra would give an idea on the uncertainty and variability of the marker spectra.

We have now added the reference mass spectra to the supplement. We show the most frequent spectra types (clusters) for each substance. This illustrates the variability of the mass spectra that are obtained from one particle type.

We consider standard deviations of the averaged mass spectra not as an ideal estimate of the uncertainty, because the abundance of a marker peak is the main criterion, not its height in the mass spectrum.

- Related to the above – how were the marker peaks identified? Given the overlap of marker peaks between different particle types, it seems to me that presenting the data as marker spectra would almost make more sense. How important are the individual markers for identification as opposed to the whole spectrum? In Table 3 you give the ratio of the number of spectra containing marker peaks (all marker peaks? just some?) to all spectra of a particular particle type. A better way to present uncertainties would be the standard deviation of the avergaed spectra (see above). The ratios in Table 3 are fairly low, I thus expect a relatively high scatter of spectra per particle type.

As already mentioned above, we included the reference spectra in the supplement. The scatter of spectra per particle type is illustrated by showing the main spectra types (clusters).

Regarding the overlap of marker peaks: It is the combination of the characteristic marker peaks that is used to assign a mass spectrum to a certain particle type. In cases where there is a complete overlap of all marker peaks between reference spectra, we can't distinguish these substances. As said above, the standard deviation of the averaged mass spectra are not the best estimate of uncertainty, because the abundance of the peak is more important that its height.

- More information should be given on the choice of clustering algorithm and the uncertainties of its outcome. There are a lot of references given to Roth (2014, 2016), but the main points should be conveyed to the reader in the manuscript (also in Table 1). A general result I infer from the ambient measurements is that secondary (here in the sense of formed from a chemical reaction/in combustion) components (both organic and inorganic) or particles containing a lot of secondary (organic) components (e. g. biomass burning) are less effective ice nuclei than primary organic particles such as e. g. biological particles. In this simple categorization, however, it is hard to place the engine exhaust particles. It would be helpful if the engine exhaust and PAH particle types were discussed in the manuscript (which is not the case now).

We have included a general explanation of the clustering and of the chosen algorithm to section 2.2 (as requested also by Reviewer #1). We also added a discussion on PAH and engine exhaust particles.

Changes to the text describing the clustering (Section 2.2):

Basically, a clustering algorithm tries to find the optimum number of clusters (i.e. groups of mass spectra) that represent the particle population by their average mass spectrum. By nature of the aerosol particle diversity and the non-uniform ionization in laser ablation ionization, it can't be expected that all particles contained in a cluster equal the average cluster spectrum (Hinz et al., 1999). Rather, each spectrum is assigned to that cluster where the distance metric

(in our case one minus Pearson's correlation coefficient r) of the single particle spectrum and the averaged cluster spectrum reaches a minimum. The fuzzy c-means algorithm differs from the k-means in that way that it accounts for the possibility that one particle may belong to two (or more) clusters by using membership coefficients, whereas the k-means assigns each spectrum strictly to that cluster where correlation with the averaged spectrum is highest.

Here we applied the fuzzy c-means algorithm because sensitivity tests conducted in the framework of a PhD thesis (Roth, 2014) with laboratory-generated particle of known composition and number have shown that the fuzzy c-means better separates the particle types and suffers less from false assignments. Also, various parameters that influence the clustering result where tested by Roth (2014), resulting in a "best choice" that was applied here as well: All mass spectra were normalized to reduce the influence of total signal intensity, and all m/z peaks were taken to the power of 0.5 to reduce the influence of the non-uniform laser ablation ionization, thereby increasing the influence of smaller peaks and decreasing that of larger signals. The "fuzzifier", a weighting exponent used for the calculation of the membership coefficients (Bezdek, 1982; Roth et al., 2016) was set to 1.2. A high number of start clusters was chosen to assure that also rare spectra types are considered in the data evaluation (for instance for the out-of-cloud data set from the JFJ campaign 2013 a number of 200 cluster was chosen; for a known particle composition as sampled during the laboratory studies a number of 10 to 50 cluster was chosen depending on the number of spectra). The start clusters were chosen randomly from the total particle population, under the condition that the correlation coefficient (r) between two randomly picked start spectra is less than 0.7. The procedure leading from the clustering algorithm to a certain number of particle types, as illustrated in Fig. 1, was as follows: After mass calibration, the spectra were clustered using the fuzzy c-means algorithm, yielding a certain number of clusters. The resulting cluster number can be lower than the chosen number of start clusters. If this is the case, the number of start clusters was sufficiently high not to suppress rare spectra types. Each cluster includes a certain number (≥ 1) of mass spectra based on the calculated membership and distance. From all mass spectra in a cluster an average spectrum is calculated which is used for the identification of the particle type represented by each cluster. All mass spectra which did not fulfill the distance criterion ($1 - r \leq 0.3$) compared to any of the clusters were sorted in the cluster "others". The averaged spectra of each cluster were manually examined with respect to the presence of the marker peaks derived from the reference mass spectra (Section 3.1) and assigned to a certain particle type. The "others" cluster was processed again using the fuzzy c-means algorithm, but with reduced constraints and again the resulting clusters were manually examined and, if possible, assigned to particle types. At the end all clusters of the same particle type were merged, whereas clusters that could not be assigned to a certain particle type were added to the cluster "others".

Changes to text with respect to PAH and engine exhaust particles (section 3.2.1):

The particle types that were assigned to the type "engine exhaust" also show C_n-fragmentation ($C_1^+ - C_5^+$, m/z 12 … 60) but can be distinguished by the peak at m/z 40 (Ca^+) which was observed in the reference mass spectra but also previously by other researchers (Vogt et al., 2003).

PAH containing particle were identified through the corresponding reference spectra and marker peaks from the laboratory studies, namely 50/51 ($C_4H_2/_3^+$), 63 ($C_5H_3^+$), 77 ($C_6H_5^+$), and

91 ($C_7H_7^+$). Even though cigarette particles (before inhalation) contain these markers as well, our reference spectra indicate that these two particle types can be distinguished because cigarette smoke additionally contains a C_n pattern (m/z 12 – 36).

I am confused about the similarity of sea salt and cooking emissions fragmentation pattern. How were the sea salt particles produced, what kind of cooking emissionswere investigated? The variety in cooking activities is incredibly large (food cooked?what method? fuel used? etc.), and without further information a “cooking spectrum”is not very meaningful.

The similarity in the fragmentation pattern of sea salt and cooking emissions only holds for the cations. Unfortunately, only cations were available from the Jungfraujoch field data (as explained in section 2.4.1). The cation spectra (with m/z 23, 39, 46, 81, 83, 139) occur both in sea salt and in barbecue emissions, and we assume that they are from salt contained in the spicing of the meat and the cheese.
In Table 2 (now Table 1) we noted that we sampled the particles directly from a barbecue (charcoal) in outside air. We used sausages, steaks and cheese. The marker peaks listed in Table 3 (now Table2) were found in all three spectra types. We will add this information to Section 2.3 and will refer to this particle type as "cooking/barbecue emissions" throughout the whole text in the revised version.
The sea salt particles were produced atomizing a solution of commercially (Sigma Aldrich) available sea salt.

Soil dust and minerals are categorized as “natural” aerosol, in accordance with classifications in literature. However, soil dust aerosol concentrations can directly be influenced by anthropogenic activities (e. g. farming, mining, forestry).These are all important factors, especially when looking into/modelling anthropogenic influences on climate via aerosol-cloud interactions. I am fully aware that soil dust source apportionment lies outside the scope of this paper, but I suggest leaving out the word “natural” and potentially add a sentence on this issue.

We agree with the reviewer and have left out the word "natural" when describing the dust particles. However, biological particles can be attributed to natural sources. We therefore refer to "primary and/or natural sources", and added a brief explanation of the different source types at the beginning of section 3.2.2:

In comparison to the out-of-cloud aerosol the IPR ensemble shows a higher number fraction of particles from primary and/or natural sources. We attribute biological and sea salt to primary natural sources, whereas soil dust and minerals emissions can directly be influenced by anthropogenic activities and can therefore not be regarded as purely natural. Biomass burning particles generated from forest fires are not primary particles, but can be related to natural sources as well.

Specific comments

P. 3 - 4, l. 37 – 2: Please give the reason for choosing the fuzzy c-means algorithm over the other two possibilities.

As mentioned above, we included a general explanation of the clustering and of the chosen algorithm to section 2.2.:

Basically, a clustering algorithm tries to find the optimum number of clusters (i.e. groups of mass spectra) that represent the particle population by their average mass spectrum. By nature of the aerosol particle diversity and the non-uniform ionization in laser ablation ionization, it can't be expected that all particles contained in a cluster equal the average cluster spectrum (Hinz et al., 1999). Rather, each spectrum is assigned to that cluster where the distance metric (in our case one minus Pearson's correlation coefficient r) of the single particle spectrum and the averaged cluster spectrum reaches a minimum. The fuzzy c-means algorithm differs from the k-means in that way that it accounts for the possibility that one particle may belong to two (or more) clusters by using membership coefficients, whereas the k-means assigns each spectrum strictly to that cluster where correlation with the averaged spectrum is highest.

Here we applied the fuzzy c-means algorithm because sensitivity tests conducted in the framework of a PhD thesis (Roth, 2014) with laboratory-generated particle of known composition and number have shown that the fuzzy c-means better separates the particle types and suffers less from false assignments.

P. 5, l. . 3 – 9: See general comment on uncertainties and limitations of marker/spectra identification.

We added the description of the error estimation and included the error ranges in the tables and throughout the text.

Changes to text (section 2.2)

The uncertainties reported along with these numbers were estimated by manual inspection of a subset of the data, as described in Roth et al. (2016). The assignment of a certain cluster to a particle type is based on the presence of the reference marker peaks in the averaged cluster mass spectrum. Upon inspection of all mass spectra in one cluster it may occur that the marker peaks (or not all of the marker peaks) are not present in an individual mass spectrum. Such a mass spectrum has nevertheless been correctly (from a mathematical point of view) assigned to the cluster by the algorithm, because the overall correlation of the mass spectrum with the cluster average is sufficiently high ($r > 0.7$). This can especially occur in cases when many other peaks are similar, as is often observed for organic particles.

For the error estimation, such particle mass spectra were regarded as "uncertain assignments". The percentage of such uncertainly assigned mass spectra was regarded as the relative error. Of the out-of-cloud data set we inspected two clusters, one assigned to biological particles (338 particles) and one assigned to biomass burning aerosol (473 particles). It turned out that 52 of the 338 inspected "biological" mass spectra (15%), and 48 of the 473 inspected "biomass burning" mass spectra (10%) had to be considered as uncertain. Thus, we conservatively estimated the relative error to be about 15% and generalized this error for whole out-of-cloud data set.

For the IPR data set, where the absolute numbers of particles are much lower, it was possible to do a more detailed inspection of the clusters: We inspected one cluster assigned to biological particles, where we found that 28 out of 76 were uncertain (37%), and one cluster of the "PAH/soot" particle type, where 9 out of 23 spectra were uncertain (40%). Those particle types containing only a small number of particles ("industrial metals", "Na + K", "aged material") were completely inspected manually, yielding uncertainties for the "industrial metals" of 14%, of the "Na + K" type of 0% (no uncertain particles), and of the "aged material" type of 44%. Thus, we estimated the relative error (from uncertain particle type assignment) of the IPR population to be 40% with the exception of the industrial metals (14%) and the "Na + K" type.

These error estimates are conservative upper limits for the error range, because the reference laboratory measurements have shown that, e.g., not all biological particles contain the characteristic marker peaks. It may therefore well be that mass spectra that are similar to the cluster average spectrum of a "biological particle" type are really biological particles, even if they do not contain the marker peaks. The uncertainty inferred from manual inspection was combined with the Poisson counting statistics error (by error propagation) for each particle type.

P. 5, l. 25 – 28: Was the inlet heated to 20_C to prevent condensation? Did you perform any assessment of the influence of the heating on the chemical composition (e. g. evaporation of semi-volatile material)? What was the residence time in the inlet? The evaporation of semi-volatile material could be especially important for SIA and SOA. Were parts of the ICE-CVI heated as well? Please add more information on sampling/inlet conditions.

Weingartner et al (1999) describe the inlet and give two reasons for heating the inlet:

"Therefore the main inlet at the Sphinx observatory was designed to sample the interstitial aerosol as well as the activated droplets. The inlet consists of a heated and insulated vertical stainless-steel tube (length: 200 cm; diameter: 6 cm) and a heated snow-hood. The temperature of the sampled air was measured 15 cm downstream of the inlet entrance and was electronically regulated to +20°C. As already mentioned, heating was necessary (1) to dry essentially all activated droplets as early as possible to reduce transmission losses and (2) to prevent riming of the inlet system during harsh conditions, especially in winter."

We can therefore refer to the Weingartner-Paper for details of the inlet and it is not necessary to repeat this information in our manuscript.

The Ice-CVI was not heated (see Mertes et al., 2007). We did not assess the influence of the heating of the total inlet on the chemical composition, and we can't think of a method that allows for doing this. But, if heating of the total led to a loss of SIA and SOA, it would result in an underestimation of particles of the type "aged material" in the out-of-cloud aerosol. This would not affect the finding that the number fraction of "aged material"-particles is much smaller in IPR than in out-of-cloud aerosol.

P. 5, l.34: What about the transmission of particles with diameters larger than 500 nm? A relatively large fraction of the particles measured at Jungfraujoch was larger than

500 nm, according to Figure 3.

The transmission decreased from 99% to 95 between 500 and 1000 nm, thus sampling line losses are not an issue for the interpretation of the ALABAMA data. We added this information to section 2.4.1:

For both sampling lines the transmission efficiency was about 99 % for particle sizes between 200 nm and 500 nm and decreased to 95 % for particle sizes up to 1000 nm. The upper 50 %-cut-off of the Ice-CVI was at about 4900 nm and for the total inlet about 3300 nm.

P. 7, l. 7 – 8: Many of the marker mass fragments of the biological particles (especially bacteria and pollen) have negative marker mass fragments. How were they identified in ambient air where you only had positive spectra?

In the positive spectra we used the peaks at m/z 47 (PO^+) and at m/z 58 ($C_3H_8N^+$) and 59 ($C_3H_9N^+$), the latter two indicating trimethylamine. We named this particle type "biological/amine".

P. 9, l. 31 – 38: See general comment above. A more thorough discussion on the properties and uncertainties of engine exhaust and PAH spectra in comparison with biomass burning spectra might shed some light on their differences in ice nucleation behavior.

We added a description on how PAH and engine exhaust were identified:

The particle types that were assigned to the type "engine exhaust" also show C_n-fragmentation ($C_1^+ – C_5^+$, m/z 12 … 60) but can be distinguished by the peak at m/z 40 (Ca^+) which was observed in the reference mass spectra but also previously by other researchers (Vogt et al., 2003).

PAH containing particle were identified through the corresponding reference spectra and marker peaks from the laboratory studies, namely 50/51 ($C_4H_2/_3^+$), 63 ($C_5H_3^+$), 77 ($C_6H_5^+$), and 91 ($C_7H_7^+$). Even though cigarette particles (before inhalation) contain these markers as well, our reference spectra indicate that these two particle types can be distinguished because cigarette smoke additionally contains a C_n pattern (m/z 12 – 36).

P.10, l. 34 – p. 11, l. 3: Please elaborate further on the comparison and discrepancy of OPC and ALABAMA size distributions. The size distributions shown in Figure 3 are completely different and basically do not allow to draw any conclusions. Are there no artefacts of the Sky-OPC?

We chose to include the size distribution measured with the OPC because the size distribution measured with the ALABAMA is not representative as a total number size distribution. The black lines in a) and c) show the number of analyzed particles in each size bin. From this it can be seen that the ALABAMA detection efficiency decreases for particles smaller than 400 nm. However, the relative number fraction of particle types in each class is not affected by this, as long as there are sufficient particles per size bin. It is therefore possible to apply the relative composition as a function of size to the size distribution measured by the OPC which we regard here as a "realistic" distribution. There are certainly artefacts to an optical particle counter, but this discussion is beyond the scope of our paper.

A second reason why we chose to show the size distribution measured by the OPC is the marked difference between the IPR and the out-of-cloud aerosol particles: The slope of the distribution is much steeper for the out-of-cloud aerosol, showing that larger particles are relatively more abundant in IPR than in the out-of-cloud aerosol.

We restructured the paragraph describing the size distributions and added more explanation.

P.11, l. 22 – 34: Whereas the meteorological conditions were similar for the two periods, they do no coincide in termns of time of day, which however can have large influences on (anthropogenic) emission patterns (e. g. engine exhaust, cooking: : :). Please take this into account in your data interpretations.

It was not possible to find two events with similar meteorological conditions, air mass origin and time of day. We added the following text:

Further, it has to be noted that both sampling periods differ in their sampling length and their time of day: The IPR sampling period lasted almost from midnight to noon, while the corresponding out-of-cloud sampling period lasted only 72 minutes in the afternoon. This may lead to different aerosol particle population due to different emission patterns of anthropogenic particles like engine exhaust, cooking etc. However, it was not possible to find two sampling periods having the same time of day and similar meteorological conditions and air mass origins. Also, the IPR sampling period could not be shortened because a sufficient number of particle needs to be sampled for a meaningful analysis.

P. 12, l. 27: This “conclusion” is a rather minor finding of your study (or put in different words, a potential reason for differences in composition between activated and non-activated aerosol particles that can be ruled out). This sentence should not be at the end of the results section.

We deleted this sentence here because this conclusion (scavenging does not play role) has already been discussed in section 3.2.2

P. 13, l. 1 – 28: Again, in your summary, please a add a few sentences on uncertainties and the limitation of the method concerning single particle marker spectra identification and particle type detection/identification in ambient air.

We added the following text at the beginning of the summary:

Uncertainties of the method arise from the finding that not all particle mass spectra from one particle type display the characteristic marker peaks. This is a result of the non-uniform ionization process of laser ablation particle mass spectrometry. For some particle types (pollen, sea salt, cooking/barbecue emissions) the fraction of mass spectra showing characteristic marker peaks was high (60 – 84 %), whereas for mineral particles (desert dust, soil dust etc.) the percentage of reference mass spectra with specific markers peaks was markedly lower (20 – 37 %). The resulting particle assignment to particle types can't be corrected for this effect, but it is likely that this is the cause for the large fraction of "unknown" particles (17 – 19 %).

Technical comments

P. 1, l. 19 – 21: “As outcome: : :” – weird sentence structure, rephrase

We rephrased to: "The outcome of these laboratory studies was characteristic marker peaks for each investigated particle type. These marker peaks were applied to the field data."

P. 1, l. 32: “and” instead of “an”

This was meant to be "an". We added a comma behind "clouds", maybe this helps:

"Depending on their chemical and microphysical properties aerosol particles have a strong impact on the solar radiation budget, an influence on the life-time of clouds, and hence also on precipitation."

P. 4, l. 37: Phrase structure; should read “Coating experiments were also…”

Changed.

P.7, l. 4 – 5: Weird sentence structure

We do not see why this sentence is unclear.

P. 9, l. 5: Dot at the end of the sentence is missing.

Corrected.

P. 12, l. 15: Sentence structure: Should read "It has to be noted further..."

We deleted this paragraph with respect to a comment of reviewer #1.

P. 12, l. 27: conclusion

Corrected.

References

Bezdek, J. C., Ehrlich, R., and Full, W.: FCM: The fuzzy c-means clustering algorithm, Computers & Geosciences, 10, 191-203, 1984.

Hinz, K.-P., Greweling, M., Drews, F., and Spengler, B.: Data Processing in On-line Laser Mass Spectrometry of Inorganic, Organic, or Biological Airborne Particles, American Society for Mass Spectrometry, 10, 648-660, 1999.

Mertes, S., Verheggen, B., Walter, S., Connolly, P., Ebert, M., Schneider, J., Bower, K. N., Cozic, J., Weinbruch, S., Baltensperger, U., and Weingartner, E.: Counterflow Virtual Impactor Based Collection of Small Ice

Particles in Mixed-Phase Clouds for the Physico-Chemical Characterization of Tropospheric Ice Nuclei: Sampler Description and First Case Study, Aerosol Science and Technology, 41, 848-864, 2007.
Roth, A.: Untersuchungen von Aerosolpartikeln und Wolkenresidualpartikeln mittels Einzelpartikel-Massenspektrometrie und optischen Methoden, PhD thesis, University of Mainz, Germany, urn:nbn:de:hebis:77-37770, 2014.
Roth, A., Schneider, J., Klimach, T., Mertes, S., van Pinxteren, D., Herrmann, H., and Borrmann, S.: Aerosol properties, source identification, and cloud processing in orographic clouds measured by single particle mass spectrometry on a Central European mountain site during HCCT-2010, Atmospheric Chemistry and Physics 15, 24419-24472, 2016.
Vogt, R., Kirchner, U., Scheer, V., Hinz, K. P., Trimborn, A., and Spengler, B.: Identification of diesel exhaust particles at an Autobahn, urban and rural location using single-particle mass spectrometry, Journal of Aerosol Science, 34, 319-337, doi: http://dx.doi.org/10.1016/S0021-8502(02)00179-9, 2003.
Weingartner, E., Nyeki, S., and Baltensperger, U.: Seasonal and diurnal variation of aerosol size distributions (10 < D < 750 nm) at a high-alpine site (Jungfraujoch 3580 m asl), Journal of Geophysical Research-Atmospheres, 39 104, 26809-26820, 1999.

Changes by authors

Change with respect to reviewer 1

Changes with respect to reviewer 2

Changes with respect to both reviewers

On-line single particle analysis of ice particle residuals from mountain-top mixed-phase clouds using laboratory derived particle type assignment

S. Schmidt[1], J. Schneider[1], T. Klimach[1], S. Mertes[2], L.P. Schenk[2], P. Kupiszewski[3,4], J. Curtius[5], and S. Borrmann[1,6]

[1]Particle Chemistry Department, Max Planck Institute for Chemistry, 55128 Mainz, Germany
[2]Leibniz Institute for Tropospheric Research, 04318 Leipzig, Germany
[3]Laboratory of Atmospheric Chemistry, Paul Scherrer Institute, 5232 Villigen, Switzerland
[4]Now at: Department of Meteorology, Stockholm University, 10691 Stockholm, Sweden
[5]Institute for Atmospheric and Environmental Sciences, Goethe-University of Frankfurt am Main, 60438 Frankfurt, Germany
[6]Institute for Atmospheric Physics, Johannes Gutenberg University, 55128 Mainz, Germany

Correspondence to: J. Schneider (johannes.schneider@mpic.de)

Abstract. In-situ single particle analysis of ice particle residuals (IPR) and out-of-cloud aerosol particles was conducted by means of laser ablation mass spectrometry during the intensive INUIT-JFJ/CLACE campaign at the high alpine research station Jungfraujoch (3580 m a.s.l.) in January ~~-/~~February 2013. During the four week campaign more than 70000 out-of-cloud aerosol particles and 595 IPR were analyzed covering a particle size diameter range from 100 nm to 3 µm. The IPR were sampled during 273 hours while the station was covered by mixed-phase clouds at ambient temperatures between -27 °C and -6 °C. The identification of particle types is based on laboratory studies of different types of biological, mineral and anthropogenic aerosol particles. The outcome of these laboratory studies was characteristic marker peaks for each investigated particle type. These marker peaks were applied to the field data. In the sampled IPR we identified ~~The results show that the sampled IPR contain~~ a larger number fraction of ~~natural,~~ primary aerosol particles, like soil dust (13 ± 5 %) and minerals (11 ± 5 %), in comparison to out-of-cloud aerosol particles (2.4 ± 0.4 % and 0.4 ± 0.1 %, respectively). Additionally, anthropogenic aerosol particles, such as ~~like~~ particles from industrial emissions and lead-containing particles, were found to be more abundant in the IPR than in the out-of-cloud aerosol. In the ~~The~~ out-of-cloud aerosol we identified ~~contained~~ a large fraction of aged particles (31 ± 5 %), including organic material and secondary inorganics~~)~~, whereas this particle type was much less abundant (2.7 ± 1.3 %) in the IPR. In a selected subset of the data where a direct comparison between out-of-cloud aerosol particles and IPR in air masses with similar origin was possible, a pronounced enhancement of biological particles was found in the IPR.

1 Introduction

Depending on their chemical and microphysical properties aerosol particles have a strong impact on the solar radiation budget, an influence on the life-time of clouds, and hence also on precipitation (direct and indirect effect; Lohmann and Feichter, 2005). In the mid-latitudes the formation of precipitation occurs mainly via the ice phase. Ice formation can be initiated in the atmosphere either homogeneously or heterogeneously. Spontaneous freezing of cloud droplets at temperatures lower than -37 °C without any catalysts is called homogeneous freezing (Cantrell and Heymsfield, 2005). At temperatures > -37 °C only heterogeneous freezing can take place with ice nucleation particles (INP) playing the key role by initiating the freezing process. In mixed-phase clouds supercooled cloud droplets and ice crystals coexist ~~at the same time~~ at temperatures between ~~-35~~ -37 °C and 0 °C. Due to the lower saturation vapor pressure over ice compared to water, under certain thermodynamic conditions ice particles grow at the expense of the supercooled droplets (Wegener-Bergeron-Findeisen process; Findeisen, 1938).

Typically only one out of 10^5 atmospheric particles has the ability to act as an INP (Rogers et al., 1998; DeMott et al., 2010).~~, therefore the abundance of INP is low and ice nucleation is a very selective process.~~ The ability of aerosol particles to act as INP depends on the chemical and physical properties, e.g. water insolubility, particle size, existence of an ice active site (Sullivan et al., 2010), as well as the required chemical bonds and crystallographic properties.

Previous laboratory and field studies have suggested that mineral dust (in several types) is one of the most important INP (e.g. DeMott et al., 2003b; DeMott et al., 2003a; Kamphus et al., 2010; Atkinson et al., 2013; Cziczo et al., 2013; Diehl et al., 2014) partially because of~~, in part,~~ its high abundance in the atmosphere (Hoose et al., 2010a). Besides mineral dust organic material of~~from~~ anthropogenic and biological origin is also of particular importance for ice formation (DeMott et al., 2003b; Cziczo et al., 2004b) and also a major component of the atmospheric aerosol in general (Jaenicke, 2005). ~~Especially~~ Meanwhile, biological particles, (e.g. spores, fungi or bacteria) are the most efficient INP at high temperatures (Hoose et al., 2010b). Good ice nucleation ability has also been demonstrated for efflorescent salts (e.g. Abbatt et al., 2006; Wise et al., 2012) and glassy organic material (e.g. Froyd et al., 2010; Murray et al., 2010). Additionally, Tobo et al. (2014) could show that the organic material found in soil dust samples is more important for the ice nucleation ability than the mineral components. Laboratory measurements by Augustin-Bauditz et al. (2016) seem to confirm the findings of Tobo et al. (2014) ~~these findings~~. The ice nucleation ability of soot particles is currently under controversial discussion: Some studies indicated good ice nucleation ability of soot (e.g. Cozic et al., 2008; Pratt et al., 2010; Pratt and Prather, 2010), others found no correlation between IPR/INP and soot (Kamphus et al., 2010; Chou et al., 2013), whereas Cziczo et al. (2013) (for cirrus clouds) and Kupiszewski et al. (2016) (for mixed phase clouds) ha~~s~~ve shown that black carbon containing particles are depleted in IPR compared to out-of-cloud aerosol. Laboratory experiments have shown a wide spread in the nucleation onset conditions for soot and negative results (no ice nucleation) for some experiments (Hoose and Möhler, 2012).

In order to provide much-needed information on the properties of INP, this ~~The aim of the~~ study ~~presented here was the~~ sets out to investigate ~~ion of~~ the chemical composition of IPR in mixed-phase clouds. To achieve this goal, a combination of an ice-selective inlet, the Ice-CVI (Ice Counterflow Virtual Impactor; Mertes et al., 2007), and a single particle mass spectrometer, the ALABAMA (Aircraft-based Laser ABlation Aerosol Mass

spectrometer; Brands et al., 2011), was operated at the high alpine Jungfraujoch research site ~~Jungfraujoch~~ in January~~/~~ February 2013.

Inspection of the data set showed a high amount of organic aerosol in both IPR and out-of-cloud aerosol particles. In order to better understand the mass spectral signatures and to be able to assign the individual mass spectra to certain particle types, it was necessary to perform an extensive set of laboratory measurements. Different types of typical atmospheric particles such as biological, mineral and organic anthropogenic particles (with sizes roughly between 100 nm and 3 µm), were studied using single particle mass spectrometry (Kamphus et al., 2008; Brands et al., 2011). The aim of these studies was to identify instrument-specific marker peaks for each particle type. Subsequently these results were applied to the Jungfraujoch data set. The chemical composition of the out-of-cloud aerosol particles is compared to the composition of the sampled IPR and a selected cloud event is compared to an out-of-cloud period having the same air mass origin.

2 Measurements and Methods

2.1 Aerosol Mass Spectrometer

The size-resolved chemical characterization of the aerosol particles was done with the single particle mass spectrometer ALABAMA (Brands et al., 2011). The ALABAMA consists of three parts: inlet system, detection region and ablation/ionization region. An aerodynamic lens (Liu-type; Liu et al., 1995a, b; Kamphus et al., 2008) and a critical orifice form the inlet system of the ALABAMA, which transmits the particles into the vacuum system and focusses the aerosol particles to a narrow beam. At the exit of the aerodynamic lens the particles are accelerated depending on~~to~~ their particle size to a velocity of about 50 - 100 ms^{-1}. For optimal working conditions the critical orifice limits the sampling flow to 80 cm^3min^{-1} and reduces the pressure in the aerodynamic lens to 3.8 hPa. The desired lens pressure was set using a critical orifice with a variable diameter to account for the low ambient pressure at the Jungfraujoch (approx. 650 hPa).

A skimmer separates the inlet system and the detection region (second pumping region). The detection region consists of two continuous wave detection lasers (Blu-Ray laser; InGaN, 405 nm), which are orthogonal to the particle beam. The particles pass through the two laser beams and the scattered light is reflected by an elliptical mirror and detected by a photomultiplier tube (PMT). The particle velocity can be determined from the time period a particle needs to pass both detection lasers. By calibration with particles of known size the vacuum aerodynamic particle diameter (DeCarlo et al., 2004) can be determined from the velocity of the particles. Both detection lasers are also used to trigger the ablation laser (pulsed ND-YAG-Laser, 266 nm, 6 – 8 mJ per pulse, 5.2 ns per pulse, max. 21 Hz). If one particle passes both continuous laser beams the electronic control system (designed and built~~d~~ at the Max Planck Institute for Chemistry, Mainz, Germany) sends out a trigger signal to the ablation laser. Subsequently, the pulsed laser fires and vaporizes/ionizes the particle partly or completely~~,~~ ionizing a fraction of the created gas molecules at the same time. The ions are separated in the Z-shaped bipolar time-of-flight mass spectrometer (TOFWERK AG, Switzerland) by their mass-to-charge ratio (m/z) and finally detected by a microchannel plate (MCP). The ALABAMA measures particles with a vacuum aerodynamic diameter in the size range of 100 nm and 3000 nm. The most efficient detection range is between 200 nm and 900 nm.

Additionally, an optical particle size spectrometer ~~counter~~ ("Sky-OPC", Grimm, model 1.129, size diameter range (d): d > 0.25 µm, d < 32 µm, calibrated with polystyrene latex (PSL) particles, refractive index = 1.60) connected directly to the ALABAMA inlet system measures the size distribution based on the intensity of the light scattered by the particles.

2.2 Single Particle Data Evaluation

The data evaluation was done using the software package CRISP (Concise Retrieval of Information from Single Particles, Klimach, 2012), based on the software IGOR Pro (Version 6, Wave-Metrics)~~, following the procedures described in Roth et al. (2016)~~. CRISP includes mass calibration, the conversion of mass spectra into so-called "stick spectra" by integration over the peak width of the ion signals, as well as different possibilities to sort the mass spectra into groups of clusters of similar spectra.

Basically, a clustering algorithm tries to find the optimum number of clusters (i.e. groups of mass spectra) that represent the particle population by their average mass spectrum. By nature of the aerosol particle diversity and the non-uniform ionization in laser ablation ionization, it can't be expected that all particles contained in a cluster equal the average cluster spectrum (Hinz et al., 1999). Rather, each spectrum is assigned to that cluster where the distance metric (in our case one minus Pearson's correlation coefficient *r*) of the single particle spectrum and the averaged cluster spectrum reaches a minimum. The fuzzy c-means algorithm (e.g. Bezdek et al., 1984; Hinz et al., 1999; Huang et al., 2013) differs from the k-means algorithm (Hartigan and Wong, 1979; Rebotier and Prather, 2007) in that way that it accounts for the possibility that one particle may belong to two (or more) clusters by using membership coefficients, whereas the k-means assigns each spectrum strictly to that cluster where correlation with the averaged spectrum is highest.

Here we applied the fuzzy c-means algorithm because sensitivity tests conducted in the framework of a PhD thesis (Roth, 2014) with laboratory-generated particle of known composition and number have shown that the fuzzy c-means better separates the particle types and suffers less from false assignments. Also, various parameters that influence the clustering results were tested by Roth (2014), resulting in a "best choice" that was applied here as well: All mass spectra were normalized to reduce the influence of total signal intensity, and all m/z peaks were taken to the power of 0.5 to reduce the influence of the non-uniform laser ablation ionization, thereby increasing the influence of smaller peaks and decreasing that of larger signals. The "fuzzifier", a weighting exponent used for the calculation of the membership coefficients (Bezdek, 1982; Roth et al., 2016) was set to 1.2. A high number of start clusters was chosen to assure that also rare spectra types are considered in the data evaluation (for instance for the out-of-cloud data set from the JFJ campaign 2013 a number of 200 clusters was chosen; for a known particle composition as sampled during the laboratory studies a number between 10 and 50 clusters was chosen depending on the number of spectra). The start clusters were chosen randomly from the total particle population, under the condition that the correlation coefficient (*r*) between two randomly picked start spectra is less than 0.7. The procedure leading from the clustering algorithm to a certain number of particle types, as illustrated in Fig. 1, was as follows: After mass calibration, the spectra were clustered using the fuzzy c-means algorithm, yielding a certain number of clusters. The resulting cluster number can be lower than the chosen number of start clusters. If this is the case, the number of start clusters was sufficiently high not to suppress rare spectra types. Each cluster includes a certain number (≥ 1) of mass spectra based on the calculated membership and distance. From all mass spectra in a cluster an average spectrum is

calculated which is used for the identification of the particle type represented by each cluster. All mass spectra which did not fulfill the distance criterion ($1 - r \leq 0.3$) compared to any of the clusters were sorted in the cluster "others". The averaged spectra of each cluster were manually examined with respect to the presence of the marker peaks derived from the reference mass spectra (Section 3.1) and assigned to a certain particle type. The "others" cluster was processed again using the fuzzy c-means algorithm, but with reduced constraints and again the resulting clusters were manually examined and, if possible, assigned to particle types. At the end all clusters of the same particle type were merged, whereas clusters that could not be assigned to a certain particle type were added to the cluster "others".

~~This sorting can be done by the operator or with one of the three implemented cluster algorithms: fuzzy c-means (e.g. Bezdek et al., 1984; Hinz et al., 1999; Huang et al., 2013), k-means (Hartigan and Wong, 1979; Rebotier and Prather, 2007) or minimum spanning tree (Gower and Ross, 1969). Differences between the clustering algorithm k-means and fuzzy c-means and the relevance and impact of some clustering parameters are described in detail in Roth (2014). The data presented in this work are based on evaluation with the fuzzy c-means algorithm with subsequent manual sorting. The details of the evaluation process are described in the following paragraph:~~

~~The result of the clustering depends significantly on the chosen clustering parameters, especially the selected number of start clusters. If this number is too small, rare fragmentation patterns (representing presumably a rare particle type) are possibly not found. For that reason a high number of start clusters was chosen to assure that also seldomly found fragmentation patterns are considered in the data evaluation (for instance for the out of cloud data set from the JFJ campaign 2013 a number of 200 clusters was chosen; for a known particle composition as sampled during the laboratory studies a number of 10 to 50 cluster was chosen depending on the number of spectra). After the mass calibration all spectra were clustered using the fuzzy c-means algorithm (see Table 1 for the adopted clustering parameters). Depending on the chosen clustering parameters, the algorithm yields a specific number of clusters. Each cluster includes a specific number of mass spectra based on the calculated membership and distance (Pearson correlation). From all mass spectra in a cluster an average spectrum is calculated which is used for the identification of the particle type represented by each cluster. All mass spectra which did not fulfill the distance criterion compared to any of the clusters are sorted in the "rest cluster". Afterwards, all average spectra were manually examined with respect to the presence of specific peaks (marker peaks), which help to identify the particle type. At the end all clusters of the same particle type were merged.~~

We report the absolute number of particles of the particle type in a certain time period and the percentage of these particles relative to the total particle population (i.e, the sum of all particle types) measured during the same time period. The uncertainties reported along with these numbers were estimated by manual inspection of a subset of the data, as described in Roth et al. (2016). The assignment of a certain cluster to a particle type is based on the presence of the reference marker peaks in the averaged cluster mass spectrum. Upon inspection of all mass spectra in one cluster it may occur that the marker peaks (or some of the marker peaks) are not present in an individual mass spectrum. Such a mass spectrum has nevertheless been correctly (from a mathematical point of view) assigned to the cluster by the algorithm, because the overall correlation of the mass spectrum with

the cluster average is sufficiently high ($r > 0.7$). This can especially occur in cases when many other peaks are similar, as is often observed for organic particles.

For the error estimation, such particle mass spectra were regarded as "uncertain assignments". The percentage of such uncertainly assigned mass spectra was regarded as the relative error. Of the out-of-cloud data set we inspected two clusters, one assigned to biological particles (338 particles) and one assigned to biomass burning aerosol (473 particles). It turned out that 52 of the 338 inspected "biological" mass spectra (15%), and 48 of the 473 inspected "biomass burning" mass spectra (10%) had to be considered as uncertain. Thus, we conservatively estimated the relative error to be about 15% and generalized this error for the whole out-of-cloud data set.

For the IPR data set, where the absolute number of particles is much lower, it was possible to do a more detailed inspection of the clusters: We inspected one cluster assigned to biological particles, where we found that 28 out of 76 were uncertain (37%), and one cluster of the "PAH/soot" particle type, where 9 out of 23 spectra were uncertain (40%). Those particle types containing only a small number of particles ("industrial metals", "Na + K", "aged material") were completely inspected manually, yielding uncertainties for the "industrial metals" of 14%, of the "Na + K" tape of 0% (no uncertain particles), and of the "aged material" type of 44%. Thus, we estimated the relative error (from uncertain particle type assignment) of the IPR population to be 40% with the exception of the industrial metals (14%) and the "Na + K" type.

These error estimates are conservative upper limits for the error range, because the reference laboratory measurements have shown that, e.g., not all biological particles contain the characteristic marker peaks. It may therefore well be that mass spectra that are similar to the cluster average spectrum of a "biological particle" type are really biological particles, even if they do not contain the marker peaks. Finally, the uncertainty inferred from manual inspection was combined with the Poisson counting statistics error (by error propagation) for each particle type.

Typically, the assignment of mass spectra to a certain particle type relies on the most abundant marker peaks. Therefore, smaller species that are abundant on many or even all particle types might go unnoticed. This is most likely the case for secondary inorganics (sulfate, nitrate) and secondary, oxygenated organics, which may add a coating to mineral dust particles, but the particle signal is still dominated by the mineral dust signatures. Thus it has to kept be kept in mind that a particle type called "mineral" should be read as "mineral-dominated". The only exception we made here is the particle type "lead-containing" where we explicitly state that lead does not represent the whole particle composition. Such a classification of particles is very common in the single particle mass spectrometry literature. The ALABAMA uses a 266 nm ND:YAG laser for particle ablation and ionization, thus we expect the assignment of mass spectra to be similar to other instruments using the same laser wavelength (e.g., ATOFMS, SPASS) of which many results on the abundance of particle types similar to our classification have been reported (Pastor et al., 2003; Erdmann et al., 2005; Hinz et al., 2006; Pratt et al., 2009; Kamphus et al., 2010; Pratt and Prather, 2010; Sierau et al., 2014).

2.3 Laboratory measurements

Classification of the different particle types based on typical marker peaks can be done using published single particle mass spectra and the identified corresponding marker peaks from the single particle mass spectrometer literature. However, dependent on ablation laser wavelength and the energy density at the ablation point, these marker peaks are likely to be instrument-specific. Therefore a large set of laboratory reference mass spectra was recorded using the ALABAMA with the objective to determine instrument-~~al~~specific marker peaks allowing for a more precise particle type classification. These instrument-specific marker peaks are expected to be valid only for the current configuration of the instruments, because parameters like ablation laser wavelength and energy density are likely to influence the ionization efficiency and the ion fragmentation pattern. Because of the high abundance of organic material in the atmospheric aerosol from natural or anthropogenic emissions (Murphy et al., 2006; Zhang et al., 2007; Kroll and Seinfeld, 2008; Hallquist et al., 2009) the focus was put on the distinction of different types of organic material depending on their sources. Additionally, different mineral particle types were investigated in order to differentiate more unambiguously between biological and mineral aerosol (e.g. soil dust). The laboratory measurements include data recorded at the Max Planck Institute for Chemistry in Mainz and at the AIDA (Aerosol Interactions and Dynamics in the Atmosphere; Möhler et al., 2003; Saathoff et al., 2003) chamber at the Karlsruhe Institute for Technology (KIT).

The various particle types (Table 1) were generated for the measurements as suspension or as supernatant ("washing water", e.g. from pollen or bacteria), as mechanically dispersed solid particles (e.g. cellulose, minerals or ground leaves), or they were directly sampled from the source ~~produced by combustion~~ (e.g. from biomass burning, fuel exhaust, soot, cigarette smoke or cooking/barbeque emissions). No size selection of the generated particles was done before transferring the particles into the ALABAMA. Coating experiments were also ~~were~~ conducted with sulfuric acid and secondary organic aerosol (SOA; produced by ozonolysis of α-pinene) coatings on mineral dust particles to mimic atmospheric aging processes. The laboratory reference mass spectra are shown in the supplement (Fig. S1 through S20). It was found that one reference particle type produced several types of spectra which were separated using the clustering algorithm described above. The supplement lists the main clusters with the number of spectra in each cluster.

For the determination of the characteristic ~~specific~~ marker peaks only those mass spectra that represented the majority (for details see supplement) of the different fragmentation patterns were considered. Using these marker peaks biological, mineral and anthropogenic particle types can be differentiated from each other. However, it has to be taken into account that the same particle type can show different fragmentation patterns and that different particle types can also show similar fragmentation patterns. Thus, for precise identification of the particle type, simultaneous measurements of ions of both polarities (anions and cations) by the mass spectrometer is a great advantage, because in many cases the most characteristics signals are only present in one polarity (predominantly in the cation spectra).

It should be further kept in mind that the detection and ablation/ionization efficiency of the ALABAMA (and of most other single particle instruments) is not equal for all particle types. Additionally, the observation that only a fraction of each reference particle type showed the characteristic marker peaks leads to a further bias of the data. It therefore has to be emphasized that the reported particle numbers and relative abundances refer only to particles detected by the ALABAMA and not to their real abundance in the atmosphere. However, comparison between different particle populations is meaningful, because the same biases hold for all sampling periods.

2.4 Field studies in mixed-phase clouds

2.4.1 Description of the measurement site

The INUIT-Jungfraujoch campaign took place in January ~~/~~February 2013 at the High Alpine Research station Jungfraujoch in the Swiss Alps (JFJ, Sphinx Laboratory, 3580 m a.s.l; 7°59'2''E, 46°32'53''N) in the frame work of the DFG (Deutsche Forschungsgemeinschaft)-funded research unit INUIT and the Swiss National Science Foundation-funded project "Interaction of aerosols with clouds and ~~R~~radiation". It was conducted in cooperation with the CLACE-campaign (Cloud and Aerosol Characterization Experiment) which took place at the same time.

Due to the exposed mountain rim position and the altitude ~~level~~ of the Jungfraujoch the Sphinx Laboratory is mainly situated in the free troposphere in winter time (Lugauer et al., 1998), and is therefore not much affected by local and near-ground emissions. The Jungfraujoch is a col ~~located in a saddle position~~ between the mountains Mönch and Jungfrau, such that locally the air masses can arrive only from two ~~different~~ directions: From north-west over the Swiss Plateau (wind direction of approx. 315 °) or from south-east over the Inner Alps via the Aletsch Glacier (approx. 135 °) (Hammer et al., 2014). ~~During the measurement campaign the IPR were sampled out of orographic, convective and non-convective clouds.~~

IPR were sampled by the Ice-CVI from orographic, convective and non-convective clouds. Under cloud conditions the ALABAMA was connected to the Ice-CVI, whereas during cloud-free conditions, the instrument sampled through a heated total aerosol inlet (total; 20 °C; Weingartner et al., 1999). Both inlets were installed on the roof of the Sphinx Laboratory.

~~The switching between both inlets was done manually, depending on the prevailing cloud conditions.~~ Under cloud conditions the ALABAMA sampled through the Ice-CVI, whereas under cloud-free condition it was switched manually to the total aerosol inlet.

The connection to the two inlet systems limited the maximal particle size of the particles reaching the ALABAMA to approximately 3 µm. The ALABAMA sampled through ¼" stainless steel tubes with different lengths (Ice-CVI to ALABAMA: 126 cm, total to ALABAMA: 261 cm). Particle losses inside the sampling tube were calculated with a modified version of the Particle Loss Calculator (von der Weiden et al., 2009). For both sampling lines t~~T~~he transmission efficiency ~~is~~ was about 99 % for ~~a~~ particle sizes between 200 nm and 500 nm~~and increased with decreasing tube length~~ and decreased to 95 % for particle sizes up to 1000 nm. The upper 50 %-cut-off of the Ice-CVI ~~is~~ was at about 4900 nm and for the total inlet about 3300 nm.

Due to technical problems with the mass spectrometer only the cation mass spectra are available from this field deployment.

2.4.2 Ice particle residual sampling

The Ice-CVI (Mertes et al., 2007) was designed to sample small, fresh ice particles (< 20 µm) out of mixed-phase clouds. Such small ice crystals have grown only by water vapor diffusion and have an age of less than 20

seconds (Fukuta and Takahashi, 1999). Therefore, it is very likely that these ice crystals have formed in the vicinity of the inlets and had only little time to scavenge interstitial aerosol particles, such that the IPR extracted from such fresh ice crystals represent to a high degree to the original IPN (Mertes et al., 2007 and references therein). A detailed description and instrumental characterization is provided in Mertes et al. (2007), therefore the system is described here only briefly: The Ice-CVI consists of three main separation sections (omnidirectional inlet, virtual impactor (VI) and pre-impactor (PI)) and a CVI (counterflow virtual impactor). The omnidirectional inlet transfers particles with a particle size up to 20 µm from the aspired air without influences of precipitation and wind. To remove larger particles which entered the inlet system owing to precipitation or wind and to get a defined upper sampling size, the VI is located just below the inlet with an upper transmission limit of 20 µm. Particles larger 20 µm are virtually impacted while smaller particles remain in the sample~~ing~~ flow. Afterwards, ice crystals are separated from the supercooled droplets with the help of the pre-impactor (two-step separation system with 10 µm and 4 µm impaction stages). The impaction plates of the pre-impactor are not actively cooled but adopt ambient temperature which must be below 0°C to allow for mixed phase clouds to exist ~~were cooled to ambient temperatures below 0 °C~~. The small ice particles bounce off the plates and remain in the sample flow whereas the supercooled droplets freeze on the plates upon contact. The transmission efficiencies of the pre-impactor with respect to supercooled droplets and ice crystals are close to 0 % respectively 100 % (Tenberken-Pötzsch et al., 2000; Mertes et al., 2007). Subsequently, the CVI removes all particles smaller than 5 µm, i.e. the interstitial aerosol and smaller supercooled droplets and small ice crystals fragments –that are possibly still in the sampling flow. To accelerate the arriving air flow to 120 ms^{-1} the CVI is located inside a wind tunnel behind the VI and PI. This velocity is required to achieve a size cut of approximately 5 µm. Only particles with sufficient inertia are able to overcome the counterflow inside the CVI. Consequently, only ice crystals with an aerodynamic diameter between 5 µm and 20 µm are sampled. The collected ice crystals are injected into a particle free and dry air inside the CVI, where the ice is completely evaporated. The released particles are the IPR and are transferred to different measurement instruments for physical and chemical characterization.

The sampling principle of the Ice-CVI leads to an enrichment of the sampled particles, which is calculated by the flow ratio before and inside the CVI inlet.

~~The Ice-CVI samples only ice crystals smaller than 20 µm. Such small ice crystals have grown only by water vapor diffusion and have an age of less than 20 seconds (Fukuta and Takahashi, 1999). Therefore, it is very likely that these ice crystals have formed in the vicinity of the inlets and had only little time to scavenge interstitial aerosol particles, such that the IPR extracted from such fresh ice crystals represent to a high degree to the original IPN (Mertes et al., 2007 and references therein).~~

A condensation particle counter (CPC, Type 3010, TSI Inc.) is located behind the CVI and measures the INP number concentration

3 Results and Discussion

3.1 Laboratory measurements of reference particles

A summary of all investigated particles types (subdivided into three classes "biological", "mineral", and "anthropogenic") is provided in Table 2 with their characteristic ~~specific~~ marker peaks. There are certain particle types where the number of mass spectra containing characteristic ~~specific~~ and unique marker peaks is relatively low (e.g. grounded maple leaves, brown coal, desert dust and volcano dust). This results partially in high uncertainties in the identification of these particle types in ambient data

Table 2 shows that some particle types belonging to one class show similarities in their marker peaks. For instance, the biological particle types bacteria and pollen have very similar fragmentation patterns (m/z -45 ($[C_2H_5O/CHO_2]^-$), -63 (PO_2^-), -71 ($[C_4H_7O/C_3H_3O_2]^-$), -79 (PO_3^-) and 47 (PO^+); fragments of oxidized organic carbon and phosphate). Also cellulose (microcrystalline) and ground leaves exhibit similar marker peaks (m/z 18 (NH_4^+)/(H_2O^+), 30 ($[CH_4N]^+$/$[COH_2]^+$), 58 ($[C_3H_8N]^+$/$[C_3H_6O]^+$); fragments indicating an amine-like or oxidized organic structure). Thus, it is not possible to distinguish here between different types of biological aerosol particles. Nevertheless, in general the identification of biological aerosol with the help of characteristic marker peaks is possible.

Additionally, also similarities between particle types from two different classes occur: Sea salt (industrial produced; Sigma Aldrich) and particles from cooking/barbecue emissions have similar fragmentation patterns in the cation spectra (m/z 46, 81, 83, 97, fragments of sodium/potassium components).

Cigarette smoke produced in two different ways was also measured: smoldering cigarette smoke and cigarette smoke which was firstly inhaled. The particles from smoke after inhalation do not show the characteristic marker peaks that were observed for PAH particles in the laboratory study. ~~fragmentation~~ But neither type of cigarette smoke could be unambiguously identified.

It was observed that some rare fragmentation patterns from pollen and biomass burning particles show similarities within the cation spectra (only one sodium (m/z 23) and potassium (m/z 39) peak). This is most likely due to the non-uniform laser ablation and ionization process, leading to production of only those two ions.

Summarizing, it was found that in general the presence of both polarities is of great importance for an unambiguous identification of a specific particle type. Only few particle types, as for example the anthropogenically produced particle types show distinct marker peaks in the cation spectra that are sufficient for identification.

It has to be noted that matrix effects may complicate the identification of particle types by markers peaks. Here we have only analyzed pure substances (with exception of the source sampling types and the natural dust samples). But in laser ablation mass spectrometry, the ionization efficiency can be a function of the particle matrix (e.g., Gross et al., 2000) such that marker peaks of certain particle types might be less abundant in internal particle mixtures. Future studies will therefore also include reference mass spectra from various types of mixed particles.

3.2 Results on IPR composition and out-of-cloud aerosol at the Jungfraujoch

3.2.1 Identified Particle Types

Altogether 71064 background aerosol particles and 595 IPR were analyzed during 217 h and ~~measurement time and 595 IPR during~~ 111 h measurement time, respectively. For the identification of specific particle types the marker peaks that resulted from the laboratory studies were applied to the Jungfraujoch data. Although, as mentioned above, the presence of both polarities allows in general for a better classification, the application of

the marker peaks only for the cations also yielded ~~also~~ useful results, because many distinguishing characteristics are found in the cation spectra (Table 2). In this way 13 different particle types were identified. The average spectra of each particle type with the highlighted marker peaks are shown in Fig. 2.

The particle types "biomass burning" and "soot" show both the typical C_n-fragmentation (C_1 – C_7, m/z 12 … 84) and can be distinguished by the presence of the peak at m/z 39 (K^+) in the cation spectra of the particles from biomass burning.

The particle types that were assigned to the type "engine exhaust" also show C_n-fragmentation (C_1^+ – C_5^+, m/z 12 … 60) but can be distinguished by the peak at m/z 40 (Ca^+) which was observed in the reference mass spectra but also previously by other researchers (Trimborn et al., 2002; Vogt et al., 2003; Shields et al., 2007).

PAH containing particles were identified through the corresponding reference spectra and marker peaks from the laboratory studies, namely 50/51 ($C_4H_2/_3^+$), 63 ($C_5H_3^+$), 77 ($C_6H_5^+$), and 91 ($C_7H_7^+$). Even though cigarette particles (before inhalation) contain these markers as well, our reference spectra indicate that these two particle types can be distinguished because cigarette smoke additionally contains a C_n pattern (m/z 12 – 36).

Two different fragmentation patterns of biological particles were found during the campaign. One type shows the marker peaks at m/z 18, 30, 58 and 59, which indicates an amine-like or oxidized organic structure. The other one shows the marker peak at m/z 47 (PO^+).

Additionally, soil dust was identified based on the laboratory studies. It is characterized by the presence of mineral components mixed with organic, biological material (e.g. peaks at m/z 18, 30, 58 and 47 point to biological components).

The laboratory data have shown that particles produced from cooking/barbecue emissions and sea salt particles have the same cation fragmentation pattern in the positive ion spectra. Thus, both particle types cannot be distinguished in this data set and therefore were merged.

Also from the particle type "aged material" two different fragmentation patterns were found. The first one shows peaks at m/z 27 and 43 ($C_2H_3^+$ and $C_3H_7^+$; fragments of organic material related to secondary organic aerosol) with a high relative intensity. The other one shows peaks at m/z 92, 108 and 165 ($Na_2NO_2^+$, $Na_2NO_3^+$, $Na_3SO_4^+$), indicating aged sea salt processed by nitrate and sulfate containing compounds (Gard et al., 1998).

The particle type “industrial metals” is marked by peaks of metal ions typically occurring in urban or industrial emissions (e.g. m/z 51/67 (V^+/VO^+), m/z 54/56 (Fe^+), m/z 55 (Mn^+), m/z 58/60 (Ni^+), m/z 59 (Co^+) and m/z 63/65 (Cu^+) (de Foy et al., 2012)). Chromium and nickel containing particles might also originate from contamination by the stainless steel tubes. But due to the low flow velocity and the laminar flow inside the tubes the production of particles by abrasion from the tube walls through collision of the aerosol particles with the inner wall of the tubes can be neglected. Another source of such contamination might be the valves that might mechanically produce particles during opening and closing. However, such particles are expected to be detected by the mass spectrometer within a few seconds after operation of a valve which was not the case. Thus we consider these particles to be real ambient atmospheric particles.

Lead containing particles show the typical isotope pattern of lead (m/z 206, 207, 208) and are internally mixed with metallic or organic components. Previous measurements at the JFJ have shown that lead containing particles were found in the IPR (Cziczo et al., 2009; Ebert et al., 2011). However, the main component of this particle type is organic or metallic origin. Thus it can be assumed that lead is only contained in small amounts in these particles. Using data from the same experiment, Worringen et al. (2015) have shown that two types of lead particles occurred in the IPR selected by the Ice-CVI during the INUIT-JFJ campaign: large homogeneous lead particles and small particles with lead inclusions. The authors concluded that only the homogeneous lead particles are artifacts produced by mechanical abrasion from the surface of the impaction plates of the Ice-CVI. Therefore, the lead containing particles described here are not considered as artifacts of the Ice-CVI.

Mineral dust particles ("minerals") were also found in the aerosol particles sampled during the JFJ campaign. This particle type was identified based on the marker peaks from the laboratory studies as well.

The types "K dominated" and "Na + K" are subcategories of the type "other", but are not clearly assignable to a certain particle type. As we inferred from the laboratory studies both particle types could originate from biological particles (e.g. pollen) or from biomass burning. On the other hand it is also possible that the "K dominated"-type is a fragmentation pattern of an inorganic salt (e.g. K_2SO_4). An unambiguous classification of these particle types from cation spectra only is not possible.

Most of these particle types do not represent pure particles like those investigated during the laboratory studies. The particles contain also other substances (as can be seen in the mass spectra) but here the most prominent marker peaks were used to identify the dominating particle type.

The type "others" includes all spectra which could not be unambiguously identified as one of the introduced particle types. This may partly be due to missing reference spectra, such that a further extension of the reference data base will allow for an identification of particles in the "other" fraction, but also due to complex mixtures of particles that cannot be identified here, especially because the anions were not available.

3.2.2 IPR composition compared to out-of-cloud aerosol particles

Figure 3 shows the relative abundance of the identified particle types in all aerosol particles sampled out-of-cloud in comparison to all sampled IPR during all cloud periods. The table included in Fig. 3 gives the absolute number of particles per particle type, the percentage of this particle type, and (in the last column) the "enrichment factor", i.e. the percentage of the particle type found in IPR divided by the percentage found in the out-of-cloud aerosol.

In comparison to the out-of-cloud aerosol we find a higher number fraction of particles from primary and/or natural sources in the IPR ensemble. We attribute biological and sea salt to primary natural sources, whereas soil dust and minerals emissions can directly be influenced by anthropogenic activities and can therefore not be regarded as purely natural. Biomass burning particles generated from forest fires are not primary particles, but can be related to natural sources as well. Between about 43 and 50 % of the identified particle types can be attributed to primary and/or natural sources; the uncertainty range is mainly due to the inability to separate between sea salt particles and cooking/barbecue emissions. The general trend of this finding agrees with the only result so far in the literature on single particle mass spectrometric analysis of IPR from mixed phase clouds (Kamphus et al., 2010): Using two single particle mass spectrometers, they report from one instrument (SPLAT) that 57% of all IPR were mineral particles or mixtures of minerals with sulfate, organics, and nitrate. The other

instrument (ATOFMS) reported that these two particles types represent a much higher fraction (78%) of all IPR, plus additionally 8% metallic particles. However, these data sets are based on smaller numbers of particle than our study (ATOFMS 152 particles, SPLAT 355 particles), such that here variations of air mass origin and meteorological conditions can be the main reason for such differences and none of these data sets can be regarded as representative for mixed phase clouds at the Jungfraujoch in general. A recent paper by Cziczo et al. (2013) summarized their analyses of ice crystals sampled during various field studies. Although formation of cirrus clouds occurs under different conditions than ice formation in mixed phases clouds, it is interesting to compare these results as well. These data clearly show that mineral dust is the most dominant heterogeneous ice nucleus in almost all cirrus encounters, but that under homogeneous freezing conditions the upper tropospheric background aerosol particles (sulfate/organic/nitrate) as well as biomass burning particles are detected in the cirrus IPR. In our data the IPR population additionally shows a higher fraction of lead containing particles (7.4 ± 3 %), industrial metals (3.5 ± 1 %) and particles from engine exhaust (6.4 ± 3 %) in comparison to the composition of the out-of-cloud aerosol. This enrichment of lead-containing particles measured at the JFJ had already been found by Cziczo et al. (2009), Kamphus et al. (2010), and Ebert et al. (2011). The out-of-cloud aerosol shows a higher fraction of aged material (30.5 ± 5 %), combustion particles (12 ± 2 % PAH/soot and 10 ± 1.5 % biomass burning) and potassium-dominated particles (11 ± 2 %). From the absence of potassium-dominated particles as well as the absence of biomass burning particles within the IPR ensemble, together with the occurrence of the same fragmentation pattern in the laboratory data for biomass burning particles, it can be surmised that the potassium-dominated type possibly originates also from biomass burning particles. On the other hand potassium containing salts also may be the source of these particles, which are not acting as INP (Twohy and Poellot, 2005).

~~The detection of potassium in laser ablation mass spectrometry is very efficient. In a laser ablation mass spectrometer the intensity of the peaks depends on the ionization efficiency. Potassium is easily ionized, such that a small amount of potassium in a particle results in a large peak and will suppress the peak intensity of other components with lower ionization efficiencies.~~

It must be taken into account that the detection of potassium in laser ablation mass spectrometry is very efficient due to its low ionization efficiency (Gross et al., 2000; Silva and Prather, 2000), such that only a small amount of potassium in a particle results in a large ion signal.

It is unexpected ~~that the IPR ensemble contains~~ particles from engine exhaust but not particles from biomass burning are found in the IPR ensemble, because the latter are also assumed to have good ice nucleation ability (Kamphus et al., 2010; Twohy et al., 2010; Pratt et al., 2011; Prenni et al., 2012). Additionally, lead-containing particles and particles from engine exhaust were found in INP ~~composition~~ (Kamphus et al., 2010; Corbin et al., 2012). Due to the finding that the same relative abundance of the particle type "PAH/soot" is found in both particle populations (12 ± 2 % and 12 ± 5 %, respectively) and the finding that biomass burning particles as well as particles from engine exhaust show an organic fragmentation pattern, further research is necessary to determine which specific property of these particle types enables their ice nucleation ability. There are only a few comparable single particle measurements reported in the literature: Measurements with the ATOFMS (Aerosol Time-of-Flight Mass Spectrometer) at the JFJ (Cziczo et al., 2009; Kamphus et al., 2010), and also aircraft measurements over North America show an amount of 5 and 10 % lead-containing particles ~~at the~~ in out-

of-cloud aerosol (Murphy et al., 2007). However, only a minor amount of minerals and fly ash was found at the Storm Peak Laboratory (SPL; 3200 m a.sl.) in northern Colorado (DeMott et al., 2003b). In agreement with our data, measurements from SPL also show ~~also~~ organic material (e.g. biomass burning particles, aged material, and PAH/soot; see Fig. 3) as the major component ~~compound~~ of the out-of-cloud aerosol (DeMott et al., 2003b; Cziczo et al., 2004a).

The finding that the chemical composition of ~~particle abundance in~~ the IPR is different from that of ~~in~~ the out-of-cloud aerosol confirms the assumption that scavenging of interstitial aerosol particles does not contribute significantly to the sampled ~~plays only a minor role for the composition of the~~ IPR, because if interstitial particle scavenging dominated, the IPR composition would look similar to that of the out-of-cloud aerosol. The presence of aged material (in low percentage) in the IPR may be explained by aerosol scavenging, but shows the limited influence of this process on IPR composition (2.7 ± 1.3 % in IPR in contrast to 30 ± 5 % in out-of-cloud-aerosol). ~~This is what was aimed for by designing the Ice-CVI to sample only small, freshly produced ice crystals with sizes below 20 µm.~~

~~From the observation that certain particle types are enriched in the IPR ensemble whereas other are less abundant, some general statements on the ice nucleation ability of these particle types can be made:~~

~~High ice nucleation ability can be inferred for soil dust, minerals, sea salt/cooking/barbecue emissions, particles from engine exhaust, lead containing particles and industrial metals. Lower ice nucleation ability can be assumed for aged material, potassium dominated particles and particles from biomass burning.~~

In summary, our observations showed an enhanced presence of particles from soil dust, minerals, sea salt/cooking/barbecue emissions, engine exhaust, lead-containing particles and industrial metals in the IPR population compared to the out-of-cloud population. Particles from aged material, from biomass burning and potassium-dominated particles were observed to be less abundant that in the out-of-cloud aerosol.

Some ~~For those~~ particle types ~~that~~ occurred in the same percentage in the out-of-cloud aerosol and in the IPR ensemble, namely ~~as~~ PAH/soot particles and biological particles. For the latter this was unexpected, because field and laboratory studies have shown that many biological particles are efficient INP, especially at higher temperatures (Hoose and Möhler, 2012)~~, a precise statement regarding their ice nucleation ability under the prevailing meteorological conditions cannot be inferred from this data set~~. One possible explanation here is that biological particles are of minor importance due to their low abundance during wintertime at the Jungfraujoch, a hypothesis that is supported by a recent study at Jungfraujoch using light-induced fluorescence that showed that most fluorescent particles were mineral dust and not biological particles (Crawford et al., 2016). On the other hand, enrichment of biological particles in IPR during a Saharan dust event was observed at the Jungfraujoch in February 2014 (Kupiszewski et al., 2016) and also in Saharan air sampled at Izaña, Tenerife, in summer 2014 (Boose et al., 2016).

3.2.3 Size resolved analysis

As mentioned above, the ALABAMA also allows for a size resolved chemical analysis of the sampled aerosol particles. Additional size information can be obtained by the OPC that was operated in parallel to the ALABAMA at the same sampling line. Figure 4 shows the size distribution of IPR and the out-of-cloud aerosol particles analyzed by ALABAMA (a and c) and those detected by the Sky-OPC (b and d). The ALABAMA data include only particles ~~of~~for which a mass spectrum was obtained. The size distribution measured with the Sky-OPC represents all ~~registered~~ particles detected at the total inlet and the Ice-CVI, respectively.

The size distribution of the IPR analyzed by ALABAMA (Fig. 4a, right ordinates) shows in comparison to the out-of-cloud aerosol (Fig. 4b) a wider distribution, especially to the larger particles size (d > 1000 nm). It must be emphasized here that the ALABAMA size distribution is not corrected for sampling and detection efficiency, the latter being optimal around 400 nm~~does not represent the "real" ambient size distribution but is a function of the detection and ionization efficiency, which is optimal around 400 nm.~~ and therefore does not represent the "real" atmospheric particle size distribution. In contrast, we consider the size distributions measured with the Sky-OPC (Figs. 4b and 4d) as representative. They show a decrease of the particle number concentration with increasing particle diameter for particle diameters above 250 nm (the lower size cut of the Sky-OPC). According to Fig. 4b the larger sized IPR (d > 1 µm) are present at a higher fraction of the total particle number than the same sizes are in the out-of-cloud aerosol (Fig. 4d). This confirms previous findings showing that larger particles are enhanced in the IPR population (Mertes et al., 2007; Kupiszewski et al., 2016). ~~the assumption that larger particles are better INP.~~ A comparison of the absolute numbers of particles and the calculation of an activity curve is not possible, because the out-of-cloud aerosol particles and the IPR (inside clouds) were measured, per definition, at different times.

The size-resolved chemical composition of the IPR (Fig. 4a), normalized for each size bin, does not show a clear relationship between size distribution and particle type, partly caused by the low counting statistics. In the lowest size bin (100 – 200 nm) the fraction of biological and PAH/soot is highest, while mineral particles (minerals and soil dust) are enhanced in the size range between 300 nm and 800 nm. Industrial metal particle are only present in the size range from 300 nm up to approximately 1800 nm.

The size-resolved chemical composition of the out-of-cloud aerosol shows an increased number fraction of biological particles between 200 and 400 nm and larger than 1000 nm. The number of potassium-dominated particles is decreasing with particle size ~~enhanced up to about 600 nm~~ while the highest number of biomass burning particles is found in the size range from 300 nm up to 1000 nm. Thus, it is unlikely that the potassium-dominated particles originate mainly from biological particles or from biomass burning. ~~Thus, the potassium-dominated particles seem to originate more likely from biological particles or from inorganic salts than from biomass burning~~. In contrast, the number of "Na+K"-particles is enriched at higher sizes (> 500 nm), suggesting another source for this particle type.

3.2.4 Case study of a selected cloud event

The comparison of the relative abundance of all identified ~~sampled~~ particles from the out-of-cloud aerosol with that of all identified ~~sampled~~ IPR exhibits significant differences ~~between both compositions~~. However, a comparison extending over the entire data set is limited as different meteorological conditions or air mass origins are included. For a closer look at the abundance of identified particles in ~~chemical composition of~~ the out-of-

cloud aerosol and the IPR, a comparison of two shorter sample periods, representing both aerosol types, was performed. To find appropriate time periods with comparable meteorological conditions, at first temperature, relative humidity, wet-bulb temperature, and wind direction were inspected. Two closely spaced sample periods were chosen, one in clouds and the other outside, with nearly the same average temperature, relative humidity and wind direction. The meteorological parameters for the two sample periods are depicted in Fig. 5 with the corresponding air mass origin back trajectories given in Fig. 6. For this purpose the HYSPLIT model was adopted (Hybrid Single Particle Langrangian Integrated Trajectory Model, National Oceanic and Atmospheric Administration; Draxler and Rolph, 2015; Rolph, 2015) with access to the meteorological data set GDAS (Global Data Assimilation; start height: 3580 m a.s.l.; calculated time: 72 h back; start time: end of the current sampling period).

The back trajectory calculations show that the air masses of both sample periods have similar, but not completely the same origin, and –besides the two excursions to higher altitudes– also a similar altitude profile of the trajectories. The air masses arrived while rising-towards the measurement platform from north-western region via France. Further, it has to be noted that both sampling periods differ in their sampling length and their time of day: The IPR sampling period lasted almost from midnight to noon, while the corresponding out-of-cloud sampling period lasted only 72 minutes in the afternoon. This may lead to different aerosol particle population due to different emission patterns of anthropogenic particles like engine exhaust, cooking etc. However, it was not possible to find two sampling periods having the same time of day and similar meteorological conditions and air mass origins. Also, the IPR sampling period could not be shortened because a sufficient number of particles needs to be sampled for a meaningful analysis.

Figure 7 shows the abundance of identified particles in ~~composition of~~ the out-of-cloud aerosol and the IPR ensemble during these two sampling times. Although the sampling conditions during both periods were very similar, the composition of these ensembles significantly differs. The IPR ensemble shows a high content of primary and/or natural material (77 ± 35 %; biological particles, soil dust, minerals and sea salt/cooking/barbecue emissions). Besides that, also anthropogenic/industrial particles are enhanced in the IPR as the last column in Fig. 7 shows: engine exhaust by a factor of 42 (± 20), lead-containing particles by 92 (± 70) and industrial metals by a factor of 4 (± 2). In comparison to that, the out-of-cloud aerosol contains a higher fraction of particles from biomass burning (22 ± 3 %) and potassium-dominated particles (22 ± 3 %). This case study shows that the observed differences between IPR and out-of-cloud aerosol particles that were observed when looking at the whole data set (Fig. 3) cannot be explained by differences in meteorological conditions and air mass origin. The finding that primary and/or natural aerosol particles such as soil dust and minerals, but also biological particles, are enhanced in the IPR population is valid for both data sets. ~~These findings agree with the general statement that natural primary aerosol such as biological particles, soil dust or minerals serve as typical ice nucleators.~~ The large number fraction of biological particles in the IPR samples of this case study exceeds that of the total IPR sample, whereas for the out-of-cloud sample it is smaller (Fig. 3). Here the variability due to different sampling times, temperatures, and air mass origins may play a role. The high number fraction of particles from biomass burning in the out-of-cloud aerosol indicates that the air masses were most likely influenced by local emissions shortly before arrival at the measurement station, but still these biomass burning particles are not found in the IPR ensemble.

~~It has further to be noted that one air mass during the out-of-cloud sample period has a different pressure history than the others: It rose up to about 400 hPa at about 50 h (Fig. 6) prior to the measurements and rapidly descended again at 30 h prior to the measurements. A closer look at the chemical composition of the particles in this air mass shows that mostly PAH/soot particles were sampled. A possible explanation might be that the aerosol particles in this air mass were removed by cloud formation or by wet removal during the uplift, and that after the downward motion the air mass picked up the local emissions from traffic or combustion, such that in contrast to the other air masses the combustion-related particles dominate.~~

Since the differences within the particle abundance ~~chemical composition~~ of both sampling periods cannot be explained by differences in air mass origin, we assume that the difference between the out-of-cloud aerosol and the IPR ~~regarding the chemical composition~~ is mainly caused by the ice nucleation ability of the particles at the prevailing meteorological conditions during these sample periods. ~~At temperatures around -20 °C biological particles, soil dust, minerals, sea salt/cooking/barbecue emissions, PAH/soot and lead containing particles were observed within ice crystal residuals have good ice nucleation ability~~. ~~Another conclusions is that here the scavenging of interstitial aerosol particles cannot explain the observed differences in composition.~~

4 Summary

We have conducted laboratory measurements of various types of aerosol particles in order to obtain reference mass spectra for the single particle mass spectrometer ALABAMA. The results show that there are different particle classes, which can be unambiguously differentiated from each other by using characteristic ~~specific~~ marker peaks. Uncertainties of the method arise from the finding that not all particle mass spectra from one particle type display the characteristic marker peaks. This is a result of the non-uniform ionization process of laser ablation particle mass spectrometry. For some particle types (pollen, sea salt, cooking/barbecue emissions) the fraction of mass spectra showing characteristic marker peaks was high (60 – 84 %), whereas for mineral particles (desert dust, soil dust etc.) the percentage of reference mass spectra with specific markers peaks was markedly lower (20 – 37 %). The resulting particle assignment to particle types can't be corrected for this effect, but it is likely that this is the cause for the large fraction of "unknown" particles (denoted as "others") in the field results.

The derived characteristic ~~specific~~ marker peaks were applied to interpret field data where ice residuals from mixed-phase clouds were extracted by an Ice-CVI and analyzed by the mass spectrometer. The comparison of the abundance of identified particle types in ~~chemical composition of~~ the out-of-cloud aerosol particles and the IPR measured during the INUIT-JFJ campaign 2013 revealed significant differences within both ensembles. Certain particles types were found to be enriched in the IPR ensemble in comparison to the out-of-cloud aerosol. From this we can determine ambient atmospheric particle types that preferably act as ice nucleating particles under the prevailing meteorological conditions at this time. The presence of INP from ~~The high ice nucleation ability of~~ lead containing particles (Cziczo et al., 2009), minerals (e.g. Hoose et al., 2010a; Kamphus et al., 2010; Hartmann et al., 2011; Hoose and Möhler, 2012; Atkinson et al., 2013), soil dust (Tobo et al., 2014), and sea salt/cooking/barbecue emissions (Wilson et al., 2015) could be confirmed. Additionally, particles from engine exhaust (Corbin et al., 2012), and industrial metals were observed to be more frequent in IPR than in out-of-cloud aerosol. ~~can be assumed as ice active.~~ It has been also reported that particles from biomass burning are efficient ice nucleating particles (Twohy et al., 2010; Pratt et al., 2011; Prenni et al., 2012). However, during the

measurements at the JFJ 2013 no particles from biomass burning were found in the IPR ensemble. In contrast to the IPR, the ensemble of the out-of-cloud aerosol particles was dominated by aged material (31 ± 5 %) and particles produced by combustion (10 ± 1.5 % biomass burning and 12 ± 2 % PAH/soot). The size distribution of both aerosol types have shown that the relative number of particles with a larger vacuum aerodynamic diameter measured with the ALABAMA (d > 1000 nm) is higher in the IPR ensemble than in the out-of-cloud aerosol. Additionally, a comparison between both particle populations was made for two closely spaced measurement periods. Although all meteorological conditions, e.g. temperature, relative humidity and wind direction (air mass origin) were similar, the chemical composition of the IPR was found to be different to that of the out-of-cloud aerosol. In comparison to the out-of-cloud aerosol particles, the IPR mainly consist of biological particles (49 ± 20 %) and soil dust (19 ± 8 %) whereas the ensemble of the out-of-cloud aerosol particles is enriched with particles from biomass burning (22 ± 3 %) and potassium dominated particles (22 ± 3 %). Because the percentage of biological particles is similar in the out of-cloud and IPR ensembles we can conclude that biological particles are ice-active at temperatures around -20 °C (temperature range between -27 °C and -6 °C over the whole measurement campaign). On the other hand, the case study indicates also a high event-to-event variability. The high number fraction of particles from biomass burning, which are not found in the IPR, indicates an influence of local emissions. This case study confirmed that the observed general differences between particle types identified in IPR and out-of-cloud aerosol ~~aerosol particle types composition~~ is not due to different air mass origin or meteorological conditions but reflects the different ice nucleation abilities of certain atmospheric particles types. The data also show that laboratory results on the ice nucleation ability of certain particles types (e.g., mineral dust and other primary particles; Möhler et al., 2007; Hoose and Möhler, 2012; Atkinson et al., 2013; Augustin-Bauditz et al., 2014; Hiranuma et al., 2015) can at least partly be transferred to ambient atmospheric data. Some of the IPR results may be influenced by scavenging of interstitial aerosol particles by the ice crystals, but this process cannot explain the differences in the abundance of particle types ~~composition of~~ between the IPR and the out-of-cloud aerosol.

Acknowledgements

This work was supported by the DFG projects FOR 1525 (INUIT), SPP 1294 (HALO, grant ME 3524/1-2), the Max Planck Society, the European Union Seventh Framework Programme (FP7/2007-2013) under grant agreement no 2662254 (ACTRIS TNA) and the Swiss National Science Foundation (200021L 135356).

The authors gratefully acknowledge the NOAA Air Resources Laboratory (ARL) for the provision of the HYSPLIT transport and dispersion model and/or READY website (http://www.ready.noaa.gov) used in this publication.

We would like to thank Swiss Meteorological Institute (MeteoSwiss) for providing meteorological measurements and the International Foundation High Altitude Research Station Jungfraujoch and Gornergrat (HFSJG) for the opportunity to perform experiments at the Jungfraujoch. Additional thanks go to Oliver Appel (MPIC Mainz) for help with the OPC data evaluations, to Oliver Schlenczek (University Mainz) for cloud observation at the JFJ and to Udo Kästner (TROPOS) for his help during the measurements at the JFJ.

References

Abbatt, J. P., Benz, S., Cziczo, D. J., Kanji, Z., Lohmann, U., and Möhler, O.: Solid ammonium sulfate aerosols as ice nuclei: a pathway for cirrus cloud formation, Science, 313, 1770-1773, 2006.

Atkinson, J. D., Murray, B. J., Woodhouse, M. T., Whale, T. F., Baustian, K. J., Carslaw, K. S., Dobbie, S., O'Sullivan, D., and Malkin, T. L.: The importance of feldspar for ice nucleation by mineral dust in mixed-phase clouds, Nature, 498, 355-358, 2013.

Augustin-Bauditz, S., Wex, H., Kanter, S., Ebert, M., Niedermeier, D., Stolz, F., Prager, A., and Stratmann, F.: The immersion mode ice nucleation behavior of mineral dusts: A comparison of different pure and surface modified dusts, Geophysical Research Letters, 41, 7375-7382, 2014.

Augustin-Bauditz, S., Wex, H., Denjean, C., Hartmann, S., Schneider, J., Schmidt, S., Ebert, M., and Stratmann, F.: Laboratory-generated mixtures of mineral dust particles with biological substances: Characterization of the particle mixing state and immersion freezing behavior, accepted by Atmospheric Chemistry and Physics, doi: doi:10.5194/acpd-15-29639-2015, 2016.

Bezdek, J. C., Ehrlich, R., and Full, W.: FCM: The fuzzy c-means clustering algorithm, Computers & Geosciences, 10, 191-203, 1984.

Boose, Y., Sierau, B., García, M. I., Rodríguez, S., Alastuey, A., Linke, C., Schnaiter, M., Kupiszewski, P., Kanji, Z. A., and Lohmann, U.: Ice nucleating particles in the Saharan Air Layer, Atmos. Chem. Phys., 16, 9067-9087, doi: 10.5194/acp-16-9067-2016, 2016.

Brands, M., Kamphus, M., Böttger, T., Schneider, J., Drewnick, F., Roth, A., Curtius, J., Voigt, C., Borbon, A., Beekmann, M., Bourdon, A., Perrin, T., and Borrmann, S.: Characterization of a Newly Developed Aircraft-Based Laser Ablation Aerosol Mass Spectrometer (ALABAMA) and First Field Deployment in Urban Pollution Plumes over Paris During MEGAPOLI 2009, Aerosol Science and Technology, 45, 46-64, 2011.

Chou, C., Kanji, Z. A., Stetzer, O., Tritscher, T., Chirico, R., Heringa, M. F., Weingartner, E., Prévôt, A. S. H., Baltensperger, U., and Lohmann, U.: Effect of photochemical ageing on the ice nucleation properties of diesel and wood burning particles, Atmos. Chem. Phys., 13, 761-772, doi: 10.5194/acp-13-761-2013, 2013.

Corbin, J. C., Rehbein, P. J. G., Evans, G. J., and Abbatt, J. P. D.: Combustion particles as ice nuclei in an urban environment: Evidence from single-particle mass spectrometry, Atmospheric Environment, 51, 286-292, 2012.

Cozic, J., Mertes, S., Verheggen, B., Cziczo, D. J., Gallavardin, S. J., Walter, S., Baltensperger, U., and Weingartner, E.: Black carbon enrichment in atmospheric ice particle residuals observed in lower tropospheric mixed phase clouds, Journal of Geophysical Research-Atmospheres, 113, D15209, 2008.

Crawford, I., Llloyd, G., Herrmann, E., Hoyle, C. R., Bower, K. N., Connolly, P. J., Flynn, M. J., Kaye, P. H., Choularton, T. W., and Gallagher, M. W.: Observations of fluorescent aerosol-cloud interactions in the free troposphere at the High-Altitude Research Station Jungfraujoch, Atmospheric Chemistry and Physics, 16, 2273-2284, 2016.

Cziczo, D. J., DeMott, P. J., Brooks, S. D., Prenni, A. J., Thomson, D. S., Baumgardner, D., Wilson, J. C., Kreidenweis, S. M., and Murphy, D. M.: Observations of organic species and atmospheric ice formation, Geophysical Research Letters, 31, L12116, 2004a.

Cziczo, D. J., Murphy, D. M., Hudson, P. K., and Thomson, D. S.: Single particle measurements of the chemical composition of cirrus ice residue during CRYSTAL-FACE, Journal of Geophysical Research-Atmospheres, 109, D04201, 2004b.

Cziczo, D. J., Stetzer, O., Worringen, A., Ebert, M., Weinbruch, S., Kamphus, M., Gallavardin, S. J., Curtius, J., Borrmann, S., Froyd, K. D., Mertes, S., Möhler, O., and Lohmann, U.: Inadvertent climate modification due to anthropogenic lead, Nature Geoscience, 2, 333-336, 2009.

Cziczo, D. J., Froyd, K. D., Hoose, C., Jensen, E. J., Diao, M., Zondlo, M. A., Smith, J. B., Twohy, C. H., and Murphy, D. M.: Clarifying the Dominant Sources and Mechanisms of Cirrus Cloud Formation, Science, 340, 1320-1324, doi: 10.1126/science.1234145, 2013.

de Foy, B., Smyth, A. M., Thompson, S. L., Gross, D. S., Olson, M. R., Sager, N., and Schauer, J. J.: Sources of nickel, vanadium and black carbon in aerosols in Milwaukee, Atmospheric Environment, 59, 294-301, 2012.

DeCarlo, P. F., Slowik, J. G., Worsnop, D. R., Davidovits, P., and Jimenez, J. L.: Particle Morphology and Density Characterization by Combined Mobility and Aerodynamic Diameter Measurements. Part 1: Theory, Aerosol Science and Technology, 38, 1185-1205, 2004.

DeMott, P. J., Sassen, K., Poellot, M. R., Baumgardner, D., Rogers, D. C., Brooks, S. D., Prenni, A. J., and Kreidenweis, S. M.: African dust aerosols as atmospheric ice nuclei, Geophysical Research Letters, 30, 1-4, 2003a.

DeMott, P. J., Cziczo, D. J., Prenni, A. J., Murphy, D. M., Kreidenweis, S. M., Thomson, D. S., Borys, R., and Rogers, D. C.: Measurements of the concentration and composition of nuclei for cirrus formation, Proceedings of the National Academy of science of the United States of America, 100, 14655-14660, 2003b.

DeMott, P. J., Prenni, A. J., Liu, X., Kreidenweis, S. M., Petters, M. D., Twohy, C. H., Richardson, M. S., Eidhammer, T., and Rogers, D. C.: Predicting global atmospheric nuclei distributions and their impacts on climate, Proceedings of the National Academy of science of the United States of America, 107, 11217-11222, 2010.

Diehl, K., Debertshäuser, M., Eppers, O., Schmithüsen, H., Mitra, S. K., and Borrmann, S.: Particle surface area dependence of mineral dust in immersion freezing mode: investigations with freely suspended drops in an acoustic levitator and a vertical wind tunnel, Atmospheric Chemistry and Physics 14, 12343-12355, 2014.

Draxler, R. R., and Rolph, G. D.: HYSPLIT (HYbrid Single-Particle Lagrangian Integrated Trajectory) Model Access via NOAA ARL READY Website (http://ready.arl.noaa.gov/HYSPLIT.php), NOAA Air Resources Laboratory, Silver Spring MD, 2015.

Ebert, M., Worringen, A., Benker, N., Mertes, S., Weingartner, E., and Weinbruch, S.: Chemical composition and mixing-state of ice residuals sampled within mixed phase clouds, Atmospheric Chemistry and Physics, 11, 2805-2816, 2011.

Erdmann, N., Dell'Acqua, A., Cavalli, P., Gruning, C., Omenetto, N., Putaud, J. P., Raes, F., and Van Dingenen, R.: Instrument characterization and first application of the single particle analysis and sizing system (SPASS) for atmospheric aerosols, Aerosol Science and Technology, 39, 377-393, doi: 10.1080/027868290935696, 2005.

Findeisen, W.: Colloidal meteorological processes in the formation of precipitation, translated from German and edited by Volken, E., Giesche, A. M., and Brönnimann, S., 2015, Meteorologische Zeitschrift, 24, 443-454, doi: 10.1127/metz/2015/0675, 1938.

Froyd, K. D., Murphy, D. M., Lawson, P., Baumgardner, D., and Herman, R. L.: Aerosols that form subvisible cirrus at the tropical tropopause, Atmospheric Chemistry and Physics, 10, 209-218, 2010.

Fukuta, N., and Takahashi, T.: The Growth of Atmospheric Ice Crystals: A Summary of Findings in Vertical Supercooled Cloud Tunnel Studies, Journal of the Atmospheric Sciences, 56, 1963-1979, 1999.

Gard, E. E., Kleeman, M. J., Gross, D. S., Hughes, L. S., Allen, J. O., Morrical, B. D., Fergenson, D. P., Dienes, T., E. Gälli, M., Johnson, R. J., Cass, G. R., and Prather, K. A.: Direct Observation of Heterogeneous Chemistry in the Atmosphere, Science, 279, 1184-1187, doi: 10.1126/science.279.5354.1184, 1998.

Gower, J. C., and Ross, G. J. S.: Minimum Spanning Trees and Single Linkage Cluster Analysis, Journal of the Royal Statistical Society, 18, 54-64, 1969.

Gross, D. S., Gälli, M. E., Silva, P. J., and Prather, K. A.: Relative Sensitivity Factors for Alkali Metal and Ammonium Cations in Single-Particle Aerosol Time-of-Flight Mass Spectra, Analytical Chemistry, 72, 416-422, doi: 10.1021/ac990434g, 2000.

Hallquist, M., Wenger, J. C., Baltensperger, U., Rudich, Y., Simpson, D., Claeys, M., Dommen, J., Donahue, N. M., George, C., Goldstein, A. H., Hamilton, J. F., Herrmann, H., Hoffmann, T., Iinuma, Y., Jang, M., Jenkin, M. E., Jimenez, J. L., Kiendler-Scharr, A., Maenhaut, W., McFiggans, G., Mentel, T. F., Monod, A., Prévot, A. S. H., Seinfeld, J. H., Surratt, J. D., Szmigielski, R., and Wildt, J.: The formation, properties and impact of secondary organic aerosol: current and emerging issues, Atmospheric Chemistry and Physics, 9, 5155-5236, 2009.

Hammer, E., Bukowiecki, N., Gysel, M., Jurányi, Z., Hoyle, C. R., Vogt, R., Baltensperger, U., and Weingartner, E.: Investigation of the effective peak supersaturation for liquid-phase clouds at the high-alpine site Jungfraujoch, Switzerland (3580 m a.s.l.), Atmospheric Chemistry and Physics, 14, 1123-1139, 2014.

Hartigan, J. A., and Wong, M. A.: Algorithm AS 136: A K-Means Clustering Algorithm, Journal of the Royal Statistical Society, 28, 200-108, 1979.

Hartmann, S., Niedermeier, D., Voigtländer, J., Clauss, T., Shaw, R. A., Wex, H., Kiselev, A., and Stratmann, F.: Homogeneous and heterogeneous ice nucleation at LACIS: operating principle and theoretical studies, Atmospheric Chemistry and Physics, 11, 1753-1767, 2011.

Hinz, K.-P., Greweling, M., Drews, F., and Spengler, B.: Data Processing in On-line Laser Mass Spectrometry of Inorganic, Organic, or Biological Airborne Particles, American Society for Mass Spectrometry, 10, 648-660, 1999.

Hinz, K. P., Erdmann, N., Gruning, C., and Spengler, B.: Comparative parallel characterization of particle populations with two mass spectrometric systems LAMPAS 2 and SPASS, International Journal of Mass Spectrometry, 258, 151-166, doi: 10.1016/j.ijms.2006.09.008, 2006.

Hiranuma, N., Möhler, O., Yamashita, K., Tajiri, T., Saito, A., Kiselev, A., Hoffmann, N., Hoose, C., Jantsch, E., Koop, T., and Murakami, M.: Ice nucleation by cellulose and its potential contribution to ice formation in clouds Nature Geoscience, 8, 273-277, 2015.

Hoose, C., Kristjánsson, J. E., Chen, J.-P., and Hazra, A.: A Classical-Theory-Based Parameterization of Heterogeneous Ice Nucleation by Mineral Dust, Soot, and Biological Particles in a Global Climate Model, Journal of the Atmospheric Sciences, 67, 2483-2503, doi: 10.1175/2010jas3425.1, 2010a.

Hoose, C., Kristjánsson, J. E., and Burrows, S. M.: How important is biological ice nucleation in clouds on a global scale?, Environmental Research Letters, 5, 024009, 2010b.

Hoose, C., and Möhler, O.: Heterogeneous ice nucleation on atmospheric aerosols: a review of results from laboratory experiments, Atmospheric Chemistry and Physics, 12, 9817-9854, 2012.

Huang, M., Hao, L., Guo, X., Hu, C., Gu, X., Zhao, W., Wang, Z., Fang, L., and Zhang, W.: Characterization of secondary organic aerosol particles using aerosol laser time-of-flight mass spectrometer coupled with FCM clustering algorithm, Atmospheric Environment, 64, 85-94, 2013.

Jaenicke, R.: Abundance of cellular material and proteins in the atmosphere, Science, 308, 73-73, 2005.

Kamphus, M., Ettner-Mahl, M., Brands, M., Curtius, J., Drewnick, F., and Borrmann, S.: Comparison of Two Aerodynamic Lenses as an Inlet for a Single Particle Laser Ablation Mass Spectrometer, Aerosol Science and Technology, 42, 970-980, 2008.

Kamphus, M., Ettner-Mahl, M., Klimach, T., Drewnick, F., Keller, L., Cziczo, D. J., Mertes, S., Borrmann, S., and Curtius, J.: Chemical composition of ambient aerosol, ice residues and cloud droplet residues in mixed-phase clouds: single particle analysis during the Cloud and Aerosol Characterization Experiment (CLACE 6), Atmospheric Chemistry and Physics, 10, 8077-8095, 2010.

Klimach, T.: Chemische Zusammensetzung der Aerosole - Design und Datenauswertung eines Einzelpartikel-Laserablationsmassenspektrometers, PhD thesis, University of Mainz, Germany, doi: urn:nbn:de:hebis:77-33547, 2012.

Kroll, J. H., and Seinfeld, J. H.: Chemistry of secondary organic aerosol: Formation and evolution of low-volatility organics in the atmosphere, Atmospheric Environment, 42, 3593-3624, 2008.
Kupiszewski, P., Zanatta, M., Mertes, S., Vochezer, P., Lloyd, G., Schneider, J., Schenk, L., Schnaiter, M., Baltensperger, U., Weingartner, E., and Gysel, M.: Ice residual properties in mixed-phase clouds at the high-alpine Jungfraujoch site, Journal of Geophysical Research: Atmospheres, doi: 10.1002/2016JD024894, 2016.
Liu, P., Ziemann, P. J., Kittelson, D. B., and McMurry, P. H.: Generating Particle Beams of Controlled Dimensions and Divergence: I. Theory of Particle Motion in Aerodynamic Lenses and Nozzle Expansions, Aerosol Science and Technology, 22, 293-313, 1995a.
Liu, P., Ziemann, P. J., Kittelson, D. B., and McMurry, P. H.: Generating Particle Beams of Controlled Dimensions and Divergence: II. Experimental Evaluation of Particle Motion in Aerodynamic Lenses and Nozzle Expansions, Aerosol Science and Technology, 22, 314-324, 1995b.
Lohmann, U., and Feichter, J.: Global indirect aerosol effects: a review, Atmospheric Chemistry and Physics, 5, 715-737, 2005.
Lugauer, M., Baltensperger, U., Furger, M., Gäggeler, H. W., Jost, D. T., Schwikowski, M., and Wanner, H.: Aerosol transport to the high Alpine sites Jungfraujoch (3454m asl) and Colle Gnifetti (4452m asl), Tellus, 50B, 76-92, 1998.
Mertes, S., Verheggen, B., Walter, S., Connolly, P., Ebert, M., Schneider, J., Bower, K. N., Cozic, J., Weinbruch, S., Baltensperger, U., and Weingartner, E.: Counterflow Virtual Impactor Based Collection of Small Ice Particles in Mixed-Phase Clouds for the Physico-Chemical Characterization of Tropospheric Ice Nuclei: Sampler Description and First Case Study, Aerosol Science and Technology, 41, 848-864, 2007.
Möhler, O., Stetzer, O., Schaefers, S., Linke, C., Schnaiter, M., Tiede, R., Saathoff, H., Krämer, M., Mangold, A., Budz, P., Zink, P., Schreiner, J., Mauersberger, K., Haag, W., Kärcher, B., and Schurath, U.: Experimental investigation of homogeneous freezing of sulphuric acid particles in the aerosol chamber AIDA, Atmospheric Chemistry and Physics, 3, 211-223, 2003.
Möhler, O., DeMott, P. J., Vali, G., and Levin, Z.: Microbiology and atmospheric processes: the role of biological particles in cloud physics, Biogeoscience, 4, 1059-1071, 2007.
Murphy, D. M., Cziczo, D. J., Froyd, K. D., Hudson, P. K., Matthew, B. M., Middlebrook, A. M., Peltier, R. E., Sullivan, A., Thomson, D. S., and Weber, R. J.: Single-particle mass spectrometry of tropospheric aerosol particles, Journal of Geophysical Research, 111, D23S32, 2006.
Murphy, D. M., Hudson, P. K., Cziczo, D. J., Gallavardin, S., Froyd, K. D., Johnston, M. V., Middlebrook, A. M., Reinard, M. S., Thomson, D. S., Thornberry, T., and Wexler, A. S.: Distribution of lead in single atmospheric particles, Atmospheric Chemistry and Physics, 7, 3195-3210, 2007.
Murray, B. J., Wilson, T. W., Dobbie, S., Cui, Z., Al-Jumur, S. M. R. K., Möhler, O., Schnaiter, M., Wagner, R., Benz, S., Niemand, M., Saathoff, H., Ebert, V., Wagner, S., and Kärcher, B.: Heterogeneous nucleation of ice particles on glassy aerosols under cirrus conditions, Nature Geoscience, 3, 233-237, 2010.
Pastor, S. H., Allen, J. O., Hughes, L. S., Bhave, P., Cass, G. R., and Prather, K. A.: Ambient single particle analysis in Riverside, California by aerosol time-of-flight mass spectrometry during the SCOS97-NARSTO, Atmospheric Environment, 37, S239-S258, doi: 10.1016/s1352-2310(03)00393-5, 2003.
Pratt, K. A., Mayer, J. E., Holecek, J. C., Moffet, R. C., Sanchez, R. O., Rebotier, T. P., Furutani, H., Gonin, M., Fuhrer, K., Su, Y. X., Guazzotti, S., and Prather, K. A.: Development and Characterization of an Aircraft Aerosol Time-of-Flight Mass Spectrometer, Analytical Chemistry, 81, 1792-1800, doi: 10.1021/ac801942r, 2009.
Pratt, K. A., and Prather, K. A.: Aircraft measurements of vertical profiles of aerosol mixing states, Journal of Geophysical Research-Atmospheres, 115, D11305, 2010.
Pratt, K. A., Heymsfield, A. J., Twohy, C. H., Murphy, S. M., DeMott, P. J., Hudson, J. G., Subramanian, R., Wang, Z., Seinfeld, J. H., and Prather, K. A.: In Situ Chemical Characterization of Aged Biomass-Burning Aerosols Impacting Cold Wave Clouds, Journal of the Atmospheric Sciences, 67, 2451-2468, 2010.

Pratt, K. A., Murphy, S. M., Subramanian, R., DeMott, P. J., Kok, G. L., Campos, T., Rogers, D. C., Prenni, A. J., Heymsfield, A. J., Seinfeld, J. H., and Prather, K. A.: Flight-based chemical characterization of biomass burning aerosols within two prescribed burn smoke plumes, Atmospheric Chemistry and Physics, 11, 12549-12565, 2011.

Prenni, A. J., DeMott, P. J., Sullivan, A. P., Sullivan, R. C., Kreidenweis, S. M., and Rogers, D. C.: Biomass burning as a potential source for atmospheric ice nuclei: Western wildfires and prescribed burns, Geophysical Research Letters, 39, L11805, 2012.

Rebotier, T. P., and Prather, K. A.: Aerosol time-of-flight mass spectrometry data analysis: a benchmark of clustering algorithms, Analytica chimica acta, 585, 38-54, doi: 10.1016/j.aca.2006.12.009, 2007.

Rogers, D. C., DeMott, P. J., Kreidenweis, S. M., and Chen, Y. L.: Measurements of ice nucleating aerosols during SUCCESS, Geophysical Research Letters, 25, 1383-1386, 1998.

Rolph, G. D.: Real-time Environmental Applications and Display sYstem (READY) Website (http://ready.art.noaa.gov), NOAA Air Resources Laboratory, Silver Spring MD, 2015.

Roth, A.: Untersuchungen von Aerosolpartikeln und Wolkenresidualpartikeln mittels Einzelpartikel-Massenspektrometrie und optischen Methoden, PhD thesis, University of Mainz, Germany, doi: urn:nbn:de:hebis:77-37770, 2014.

Roth, A., Schneider, J., Klimach, T., Mertes, S., van Pinxteren, D., Herrmann, H., and Borrmann, S.: Aerosol properties, source identification, and cloud processing in orographic clouds measured by single particle mass spectrometry on a Central European mountain site during HCCT-2010, Atmospheric Chemistry and Physics 15, 24419-24472, 2016.

Saathoff, H., Moehler, O., Schurath, U., Kamm, S., Dippel, B., and Mihelcic, D.: The AIDA soot aerosol characterisation campaign 1999, Journal of Aerosol Science, 34, 1277-1296, 2003.

Shields, L. G., Suess, D. T., and Prather, K. A.: Determination of single particle mass spectral signatures from heavy-duty diesel vehicle emissions for PM2.5 source apportionment, Atmospheric Environment, 41, 3841-3852, doi: 10.1016/j.atmosenv.2007.01.025, 2007.

Sierau, B., Chang, R. Y. W., Leck, C., Paatero, J., and Lohmann, U.: Single-particle characterization of the high-Arctic summertime aerosol, Atmos. Chem. Phys., 14, 7409-7430, doi: 10.5194/acp-14-7409-2014, 2014.

Silva, P. J., and Prather, K. A.: Interpretation of Mass Spectra from Organic Compounds in Aerosol Time-of-Flight Mass Spectrometry, Analytical Chemistry, 72, 3553-3562, doi: 10.1021/ac9910132, 2000.

Sullivan, R. C., Petters, M. D., DeMott, P. J., Kreidenweis, S. M., Wex, H., Niedermeier, D., Hartmann, S., Clauss, T., Stratmann, F., Reitz, P., Schneider, J., and Sierau, B.: Irreversible loss of ice nucleation active sites in mineral dust particles caused by sulphuric acid condensation, Atmospheric Chemistry and Physics, 10, 11471-11487, 2010.

Tenberken-Pötzsch, B., Schwikowski, M., and Gäggeler, H. W.: A method to sample and separate ice crystals and supercooled cloud droplets in mixed phased clouds for subsequent chemical analysis, Atmospheric Environment, 34, 3629-3633, 2000.

Tobo, Y., DeMott, P. J., Hill, T. C. J., Prenni, A. J., Swoboda-Colberg, N. G., Franc, G. D., and Kreidenweis, S. M.: Organic matter matters for ice nuclei of agricultural soil origin, Atmospheric Chemistry and Physics, 14, 8521-8531, 2014.

Trimborn, A., Hinz, K. P., and Spengler, B.: Online analysis of atmospheric particles with a transportable laser mass spectrometer during LACE 98, Journal of Geophysical Research: Atmospheres, 107, LAC 13-11-LAC 13-10, doi: 10.1029/2001JD000590, 2002.

Twohy, C. H., and Poellot, M. R.: Chemical characteristics of ice residual nuclei in anvil cirrus clouds: evidence for homogeneous and heterogeneous ice formation, Atmospheric Chemistry and Physics, 5, 2289-2297, 2005.

Twohy, C. H., DeMott, P. J., Pratt, K. A., Subramanian, R., Kok, G. L., Murphy, S. M., Lersch, T., Heymsfield, A. J., Wang, Z., Prather, K. A., and Seinfeld, J. H.: Relationships of Biomass-Burning Aerosols to Ice in Orographic Wave Clouds, Journal of the Atmospheric Sciences, 67, 2437-2450, 2010.

Vogt, R., Kirchner, U., Scheer, V., Hinz, K. P., Trimborn, A., and Spengler, B.: Identification of diesel exhaust particles at an Autobahn, urban and rural location using single-particle mass spectrometry, Journal of Aerosol Science, 34, 319-337, doi: 10.1016/S0021-8502(02)00179-9, 2003.

von der Weiden, S.-L., Drewnick, F., and Borrmann, S.: Particle Loss Calculator - a new software tool for the assessment of the performance of aerosol inlet systems, Atmospheric Measurement Techniques, 2, 479-494, 2009.

Weingartner, E., Nyeki, S., and Baltensperger, U.: Seasonal and diurnal variation of aerosol size distributions (10<D<750 nm) at a high-alpine site (Jungfraujoch 3580 m asl), Journal of Geophysical Research-Atmospheres, 104, 26809-26820, 1999.

Wilson, T. W., Ladino, L. A., Alpert, P. A., Breckels, M. N., Brooks, I. M., Browse, J., Burrows, S. M., Carslaw, K. S., Huffman, J. A., Judd, C., Kilthau, W. P., Mason, R. H., McFiggans, G., Miller, L. A., Najera, J. J., Polishchuk, E., Rae, S., Schiller, C. L., Si, M., Temprado, J. V., Whale, T. F., Wong, J. P., Wurl, O., Yakobi-Hancock, J. D., Abbatt, J. P., Aller, J. Y., Bertram, A. K., Knopf, D. A., and Murray, B. J.: A marine biogenic source of atmospheric ice-nucleating particles, Nature, 525, 234-238, 2015.

Wise, M. E., Baustian, K. J., Koop, T., Freedman, M. A., Jensen, E. J., and Tolbert, M. A.: Depositional ice nucleation onto crystalline hydrated NaCl particles: a new mechanism for ice formation in the troposphere, Atmospheric Chemistry and Physics, 12, 1121-1134, 2012.

Worringen, A., Kandler, K., Benker, N., Dirsch, T., Mertes, S., Schenk, L., Kästner, U., Frank, F., Nillius, B., Bundke, U., Rose, D., Curtius, J., Kupiszewski, P., Weingartner, E., Vochezer, P., Schneider, J., Schmidt, S., Weinbruch, S., and Ebert, M.: Single-particle characterization of ice-nucleating particles and ice particle residuals sampled by three different techniques, Atmospheric Chemistry and Physics, 15, 4161-4178, 2015.

Zhang, Q., Jimenez, J. L., Canagaratna, M. R., Allan, J. D., Coe, H., Ulbrich, I., Alfarra, M. R., Takami, A., Middlebrook, A. M., Sun, Y. L., Dzepina, K., Dunlea, E., Docherty, K., DeCarlo, P. F., Salcedo, D., Onasch, T., Jayne, J. T., Miyoshi, T., Shimono, A., Hatakeyama, S., Takegawa, N., Kondo, Y., Schneider, J., Drewnick, F., Borrmann, S., Weimer, S., Demerjian, K., Williams, P., Bower, K., Bahreini, R., Cottrell, L., Griffin, R. J., Rautiainen, J., Sun, J. Y., Zhang, Y. M., and Worsnop, D. R.: Ubiquity and dominance of oxygenated species in organic aerosols in anthropogenically-influenced Northern Hemisphere midlatitudes, Geophysical Research Letters, 34, L13801, 2007.

Table 1: Clustering parameter applied in the data evaluation. (For details and the meaning of the parameters see Roth, 2014)

Preprocessing type	Power each mz
Preprocessing power	0.5
Normalization type	Sum
Initialization type	Find different start cluster
Cluster difference	0.7
Distance	Correlation
Fuzzifier	1.2
Fuzzy abort	0.0001

Table 1: Investigated particles types with the corresponding generation procedure, manufacturer and purity where applicable data.

Particle type	Generation procedure	Manufacturer
Bacteria	AIDA (suspension)	
Ground leaves	AIDA (mechanically dispersed)	
Pollen	AIDA/washing-water	
Cellulose	Mechanically dispersed	Sigma Aldrich
Sea salt	Solution	Sigma Aldrich
Biomass burning	Combustion (chimney)	
Brown coal	Combustion (chimney)	
Cigarette smoke	Combustion (closed room)	
Cooking/barbecue emissions (sausage, steak ,cheese)	Directly sampled during a barbecue (courtyard)	
Engine exhaust	Directly sampled at the exhaust pipe	
PAH:	Suspension	
Benzo[ghi]perylene		Fluka (level of purity ≥ 98 %)
Triphenylene		Fluka (level of purity ≥ 98 %)
Dibenzo(a,h)anthracene		SUPLECO Analytical (99.9 % purity)
Soot	AIDA (combustion)	
Mineral	AIDA (suspension)	
Desert dust	AIDA (suspension)	
Soil dust	AIDA (suspension)	
Volcano dust	AIDA (suspension)	
Additionally investigated biological particles		
Alanine	Solution	Roth (purity ≥ 99 %)
Cysteine	Solution	Sigma Aldrich (purity 97 %)
Glutamic acid	Solution	Alfa Aesar (purity 99 %)
Leucine	Solution	Fluka (purity > 99 %)
Proline	Solution	Roth (purity ≥ 98.5 %)
Tryptophan	Solution	Roth
Valine	Solution	Roth (purity ≥ 98.5 %)
Glucose	Solution	Roth (purity ≥ 99.5 %)
Sucrose	Solution	Roth (purity ≥ 99.5 %)
Riboflavin	Suspension	Acros Organics (purity 98 %)
Chlorophyll	Suspension	Roth
Hemoglobin	Solution	Sigma Aldrich

Table 2: Overview of the different measured particle classes from primary biological, sea salt, combustion and mineral sources with their characteristic ~~specific~~ marker peaks, along with ~~and the~~ number and percentage of spectra which include these marker peaks. ~~The uncertainty (values in parentheses), as also provided, is calculated from number of spectra which include the marker peaks divided by the whole number of spectra measured of the particular particle type.~~ Peaks marked in red are the characteristic ~~specific~~ marker peaks of each particle class, peaks marked in blue show the characteristic ~~typical~~ marker peaks of one particle type. "–" designates anion spectra and "+" cation spectra.

Particle class	Particle type	Marker peaks [m/z]	Number of mass spectra with marker peaks	Comments
biological/amine	Bacteria	-: 16 [O], 26 [CN, C_2H_2], 42 [CNO, C_2H_2O, C_3H_6], **45 [C_2H_5O]**, **63 [PO_2]**, **71 [C_3H_7O, $C_3H_3O_2$]**, **79 [PO_3]**, 96 [SO_4], 97 [HSO_4] +: **23 [Na]**, 39 [K], **47 [PO]**, 56 [Fe], **97 [NaKCl, C_7H_{13}]**	1042 (42 %)	Snomax® shows no Peak at m/z +56 [Fe, CaO] and -97 [HSO_4]
	Ground maple leaves	-: 62 [NO_3], 97 [HSO_4], **125 [$H(NO_3)_2$]**, **195 [$H(SO_4)_2$]** +: C_n: 12-36, **18 [NH_4]**, 27 [Al, C_2H_3], **30 [CH_4N]**, 39 [K], **58 [C_3H_8N]**	93 (48 %)	
	Pollen	-: 26 [CN, C_2H_2], 42 [CNO, C_2H_2O, C_3H_6], **45 [C_2H_5O]**, **59 [C_3H_9N/C_3H_7O]**, 63 [PO_2], **71 [C_3H_7O, $C_3H_3O_2$]**, **79 [PO_3]**, 97 [HSO_4] +: 15 [CH_3], 23 [Na], 39 [K], 40 [Mg], 47 [PO], 58 [**C_3H_8N**], **59 [C_3H_9N, C_3H_7O]**	1277 (61 %)	Birch pollen shows additionally peaks at m/z -63 [PO_2], 23 [Na], and 56 [Fe, CaO]
	Cellulose	-: C_n: 24-48, **26 [CN, C_2H_2]**, 42 [CNO, C_2H_2O, C_3H_6], 62 [NO_3], +: C_n: 12-36, 27 [Al, C_2H_3], **40 [Mg]**, **56 [Fe, MgO]**, **113 [C_8H_{17}]**, **115 [C_9H_7, $C_7H_{15}O$]**	196 (18 %)	Microcrystalline cellulose shows different fragmentation pattern: m/z – 71 [C_3H_7O, $C_3H_3O_2$], **-125 [$H(NO_3)_2$]**, **-195 [$H(SO_4)_2$]**, **18 [NH_4]**, **30 [CH_4N]**, **58 [C_3H_8N]** (106 spectra of 454 (23 %))
sea salt	Sea salt	-: 24 [C_2], 45 [C_2H_5O], 60 [C_5] **95 [CH_3SO_3, PO_4]**, 96 [SO_4], 97 [HSO_4], **99 [$H^{34}SO_4$, $NaCO_4$, $C_6H_{11}O$]**, 135 [KSO_4], 158 [NO_3SO_4] +: **23 [Na]**, 24 [C_2, Mg], 39 [K], 40 [Ca], **46 [Na_2]**, **81 [Na_2Cl]**, **83 [Na_2Cl]**, 97 [HSO_4], **139 [$Na(NaCl)_2$]**	173 (84 %)	
Combustion	Biomass burning	-: **C_n: 24-144**, **26 [CN, C_2H_2]**, 79 [PO_3], 97 [HSO_4] +: **C_n: 12-192**, **23 [Na]**, **39 [K]**	7436 (29 %)	
	Brown coal	-: **C_n: 24-132**, 26 [CN, C_2H_2], **80 [SO_3]**, 97 [HSO_4] +: **C_n: 12-132**, **23 [Na]**, **39 [K]**	53 (54 %)	
	Cigarette smoke	-: 26 [CN, C_2H_2], 42 [CNO, C_3H_6], 46 [NO_2] +: **C_n: 12-36**, 27 [Al, C_2H_3], 39 [K], **50 [C_4H_2]**, **51 [C_4H_3]**, **63 [C_5H_3]**, **77 [C_6H_5]**, **115 [C_9H_7]**	13017 (35 %)	Measurements after smoke inhalation show no PAH-fragmentation
	Cooking/barbecue emissions	-: 26 [CN, C_2H_2], 42[CNO, C_3H_6], 46 [NO_2], 97 [HSO_4] +: 23 [Na], 39 [K], **46 [Na_2]**, **81 [Na_2Cl]**, **83 [Na_2Cl]**, **97 [NaKCl]**, **113 [K_2Cl]**	299 (60 %)	
	Engine exhaust	-: **C_n: 24-60**, 26 [CN, C_2H_2], 46 [NO_2], 62 [NO_3], 79 [PO_3], **80 [SO_3]**, 97 [HSO_4]	470 (40 %)	Incomplete combustions having weaker C_n-fragmentation and no peak at m/z -80 [SO_3]

	PAH	+: **C_n: 12-60**, 23 [Na], 27 [Al, C_2H_3], 39 [K], **40 [Ca]** -: 26 [C_2H_2], 79 [PO_3], 97 [HSO_4] +: 27 [C_2H_3], **50/51 [$C_4H_{2/3}$], 63 [C_5H_3]**, **77 [C_6H_5]**, **91 [C_7H_7]**	419 (37 %)	
	Soot	-: **C_n: 12-156**, 26 [CN, C_2H_2] +: **C_n: 12-144**	190 (41 %)	
Mineral	Minerals	-: C_n: 24-48 +: **C_n: 12-36**, **27 [Al]**, **40 [Ca]**, 48 [Ti], 50 [Cr], **56 [Fe, CaO]**	827 (22 %)	
	Desert dust	-: C_n: 24-48, 26 [CN, C_2H_2], 42 [CNO, C_3H_6], **59 [C_3H_7O, AlO_2]**, **60 [C_5, SiO_2]**, **76 [SiO_3]** +: **C_n: 12-36**, 7 [Li], **27 [Al]**, **40 [Ca]**, 48 [Ti], 54 [Fe], **56 [Fe, CaO]**, 64 [TiO]	60 (20 %)	
	Soil dust	-: 26 [CN, C_2H_2], 42 [CNO, C_3H_6), **59 [C_3H_7O, AlO_2]**, **60 [C_5, SiO_2]**, 63 [PO_2], **76 [SiO_3]**, **79 [PO_3]** +: 7 [Li], **27 [Al]**, 48 [Ti], 54 [Fe], **56 [Fe]**, 64 [TiO]	721 (33 %)	Soil dust from Switzerland „Bächli“ exhibits different fragmentation pattern in the anion spectra; cation spectra show additionally m/z 18 [NH_4], 30 [CH_4N], 58 [C_3H_8N] and only m/z 27 [Al] and 56 [Fe, CaO] of the indicated marker peaks (891 of 2122 spectra (42 %))
	Volcano dust	-: 24 [C_2], 36 [C_3], 97 [HSO_4] +: **C_n: 12-36**, 23 [Na], **27 [Al]**, 28 [Si], 39 [K], **40 [Ca]**, **56 [Fe, CaO]**	32 (37 %)	

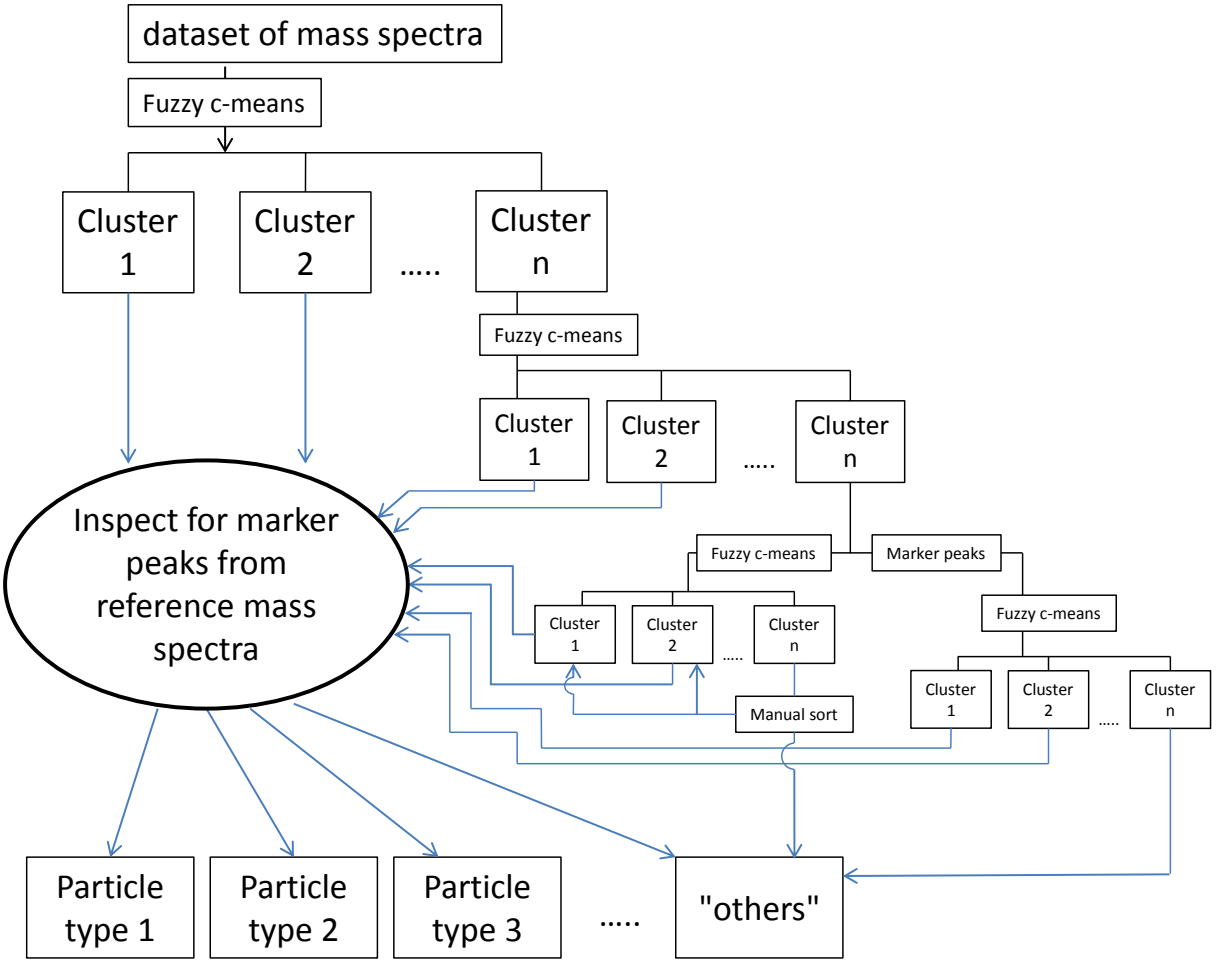

Fig. 1: Flow chart of the single particle mass spectra evaluation. Each cluster that was found by the fuzzy c-means algorithm was manually inspected for marker peaks and assigned to the appropriate particle type. This procedure was repeated with the group of mass spectra (cluster n) that did not meet the distance criterion in the first clustering run. Eventually the remaining mass spectra were manually sorted and inspected for marker peaks.

biomass burning

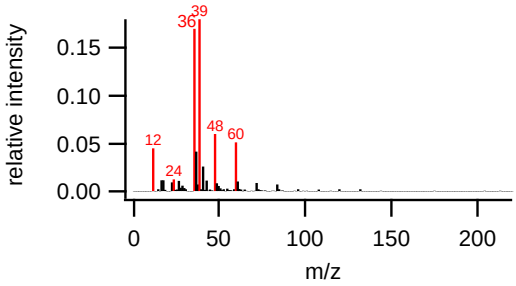

soot

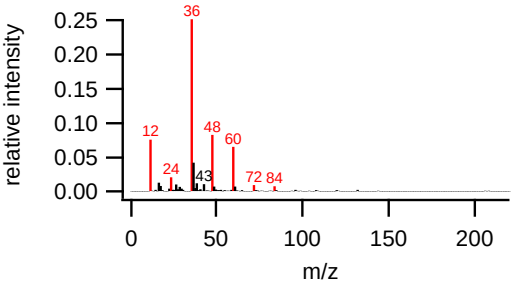

biological particles type 1

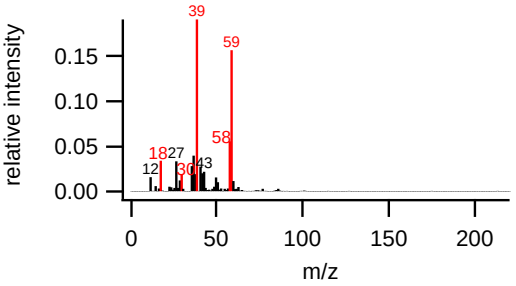

biological particles type 2

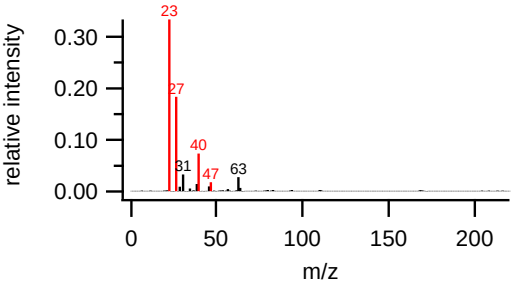

soil dust

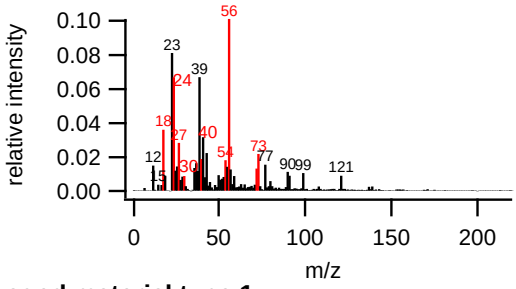

sea salt/cooking emissions

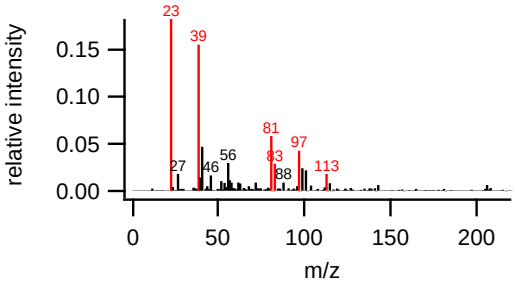

aged material type 1

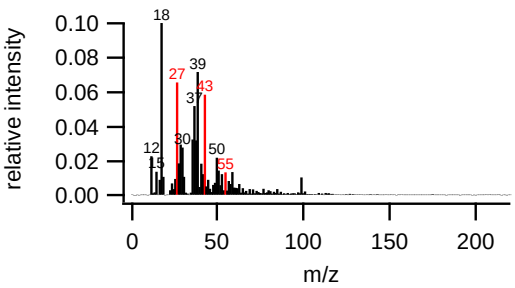

aged material type 2

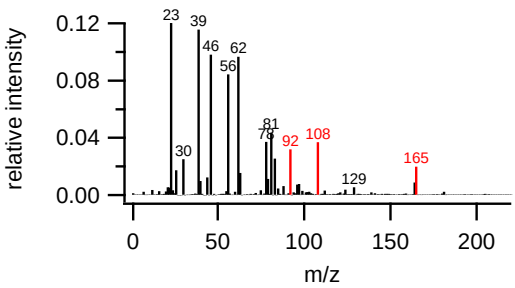

engine exhaust

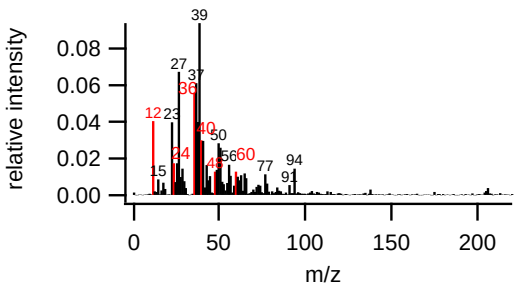

PAH

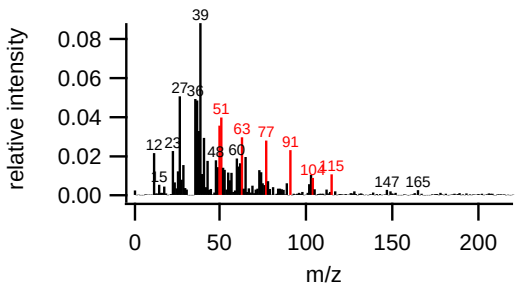

1

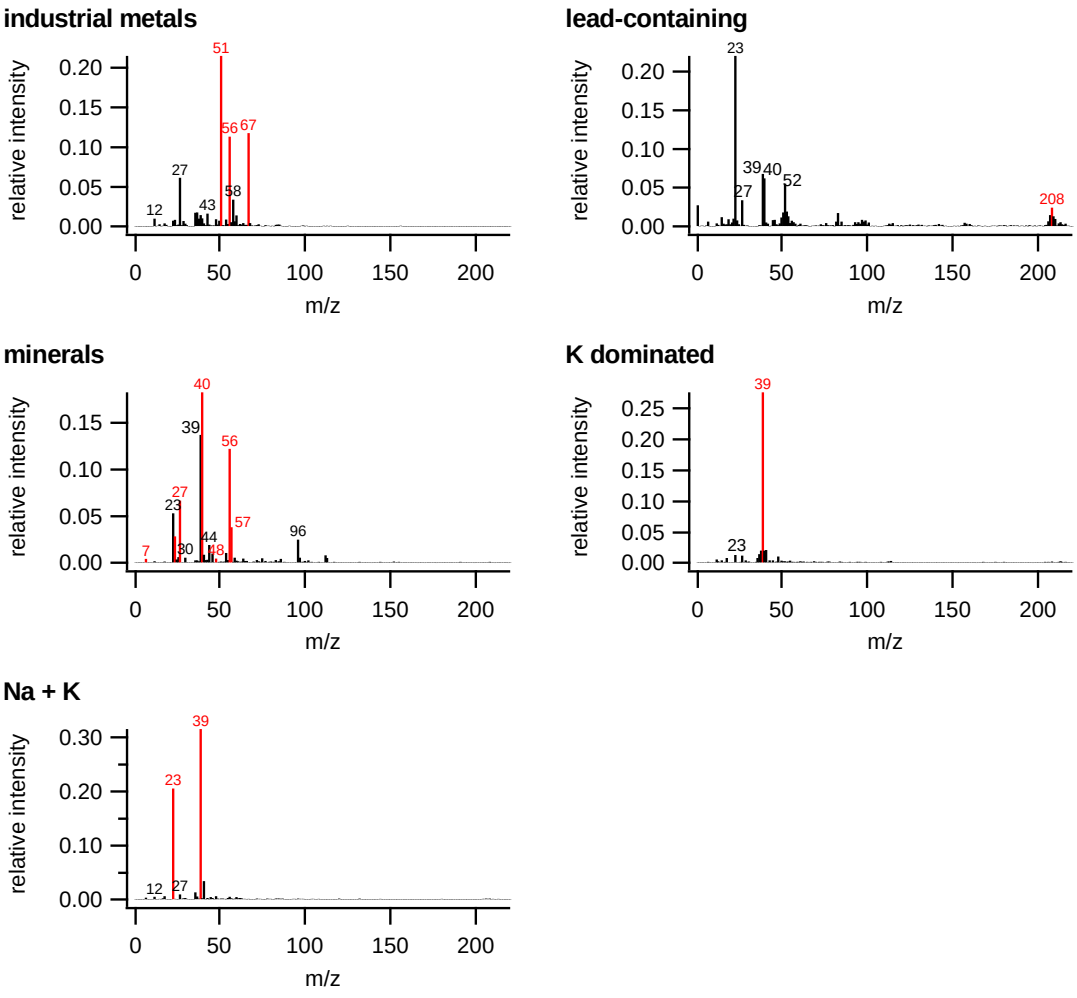

Fig. 2: Average spectra (only cations) of all identified particle types from the JFJ-measurements. The classification was done according to the results from the laboratory studies (Table 2). The red highlighted peaks indicate the marker peaks used for identification of the particle type.

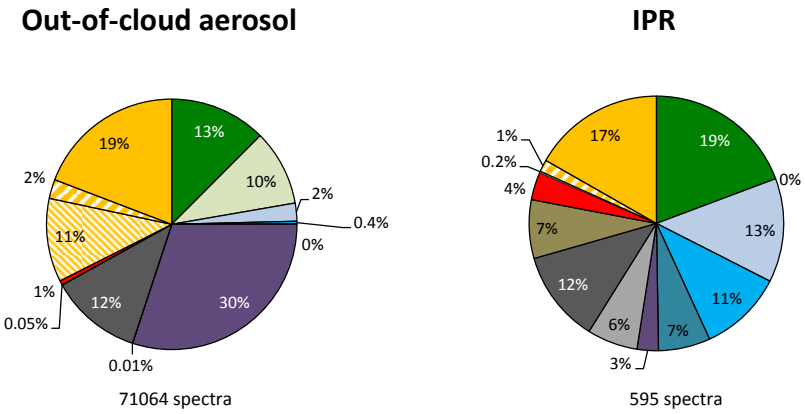

Particle type	Out-of-cloud		IPR		% IPR / % Out-of-cloud
	Total number	percentage	Total number	percentage	
biological/amine	8871 (± 1334)	12.6 (± 1.9)%	114 (± 47)	19.2 (± 7.9)%	1.5 (± 0.7)
biomass burning	6959 (± 1047)	9.9 (± 1.5)%	0	0	0
soil dust	1655 (± 251)	2.4 (± 0.4)%	78 (± 32)	13.1 (± 5.4)%	5.5 (± 2.5)
minerals	261 (± 42)	0.4 (± 0.1)%	67 (± 28)	11.3 (± 4.7)%	30 (± 14)
sea salt/cooking emissions	0	0	39 (± 17)	6.6 (± 2.8)%	--
aged material	21392 (± 3212)	30.5 (± 4.6)%	16 (± 7)	2.7 (± 1.3)%	0.09 (± 0.04)
engine exhaust	8 (± 3)	0.011 (± 0.004)%	38 (± 16)	6.4 (± 2.8)%	560 (± 320)
PAH/soot	8423 (± 1267)	12.0 (± 1.8)%	69 (± 29)	11.6 (± 4.8)%	1.0 (± 0.4)
lead-containing	36 (± 8)	0.05 (± 0.01)%	44 (± 19)	7.4 (± 3.1)%	140 (± 70)
industrial metals	399(± 63)	0.6 (± 0.1)%	21 (± 5)	3.5 (± 0.9)%	6.2 (± 1.9)
K dominated	7665 (± 1153)	10.9 (± 1.6)%	1 (± 1)	0.17 (± 0.17) %	0.02 (± 0.02)
Na + K	1756 (± 266)	2.5 (± 0.4) %	9 (± 3)	1.5 (± 0.5)%	0.6 (± 0.2)
others	13639 (± 1899)	18.0 (± 2.7)%	99 (± 41)	16.6 (± 6.9)%	0.9 (± 0.4)

Fig. 3: Relative abundance of identified particle types in all out-of-cloud particles (left) and all IPR (right). The table lists absolute number of particles with uncertainties, percentages, and "enrichment factor" (percentage IPR / percentage out-of-cloud).

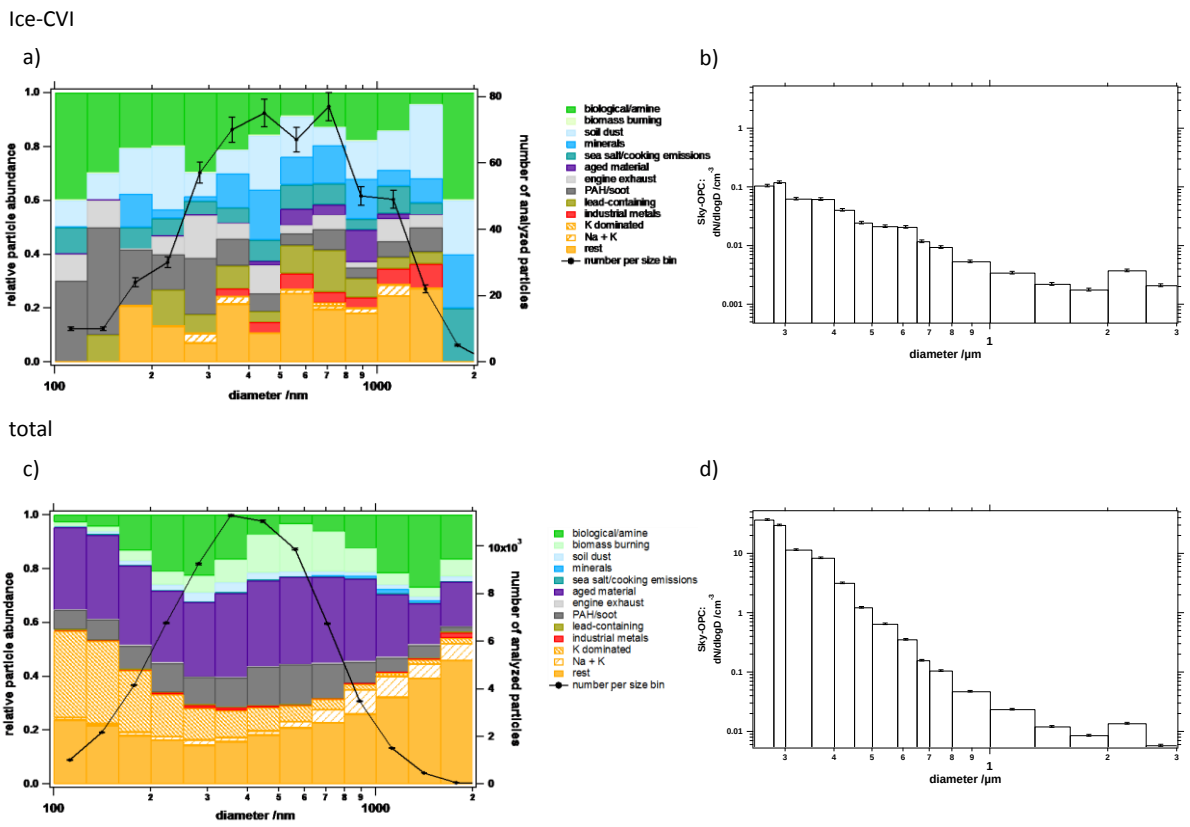

Fig. 4: Size resolved abundance of particle types ~~composition of the~~ in IPR (a)) and out of-cloud-aerosol particles (c)) sampled with the ALABAMA and the measured size distribution of the Sky-OPC (Ice-CVI: b; total: d). The black lines in a) and c) refer to the numbers of particles per size bin (right ordinate) of which a mass spectrum was obtained by ALABAMA with error bars based on counting statistics. The errors of the Sky-OPC data result from Gaussian propagation of uncertainty, including counting statistics, the manufacturer-given error of the OPC of 3 %, and the error of the enrichment factor (4 %).

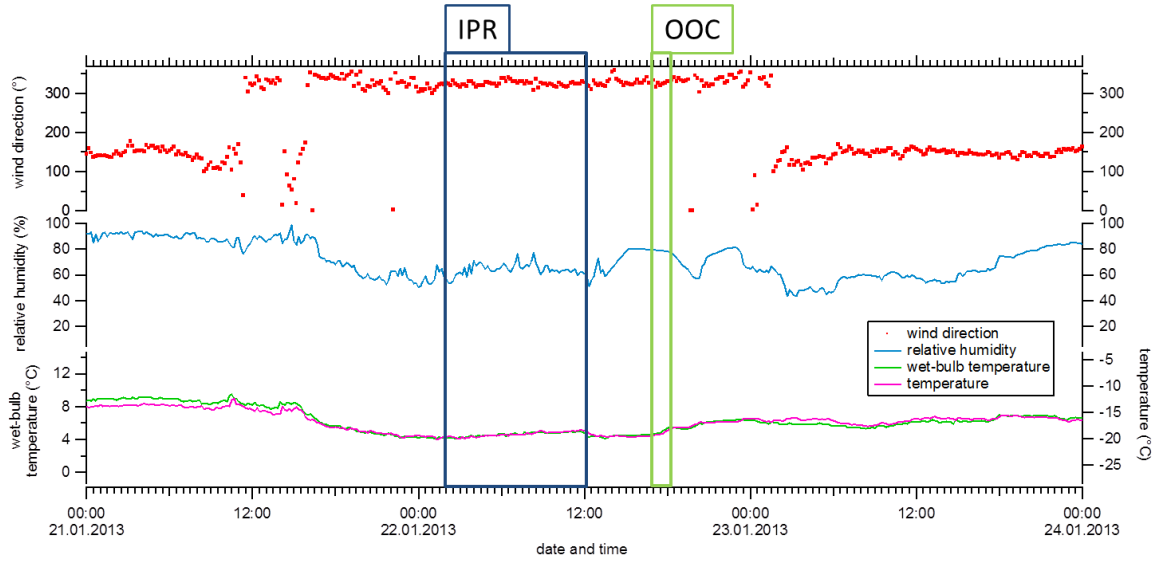

Fig. 5: Wind direction, relative humidity, potential wet-bulb temperature and temperature (data from Meteo Swiss at the JFJ). The IPR sampling period is highlighted in blue, the out-of-cloud aerosol (OOC) sampling period in green.

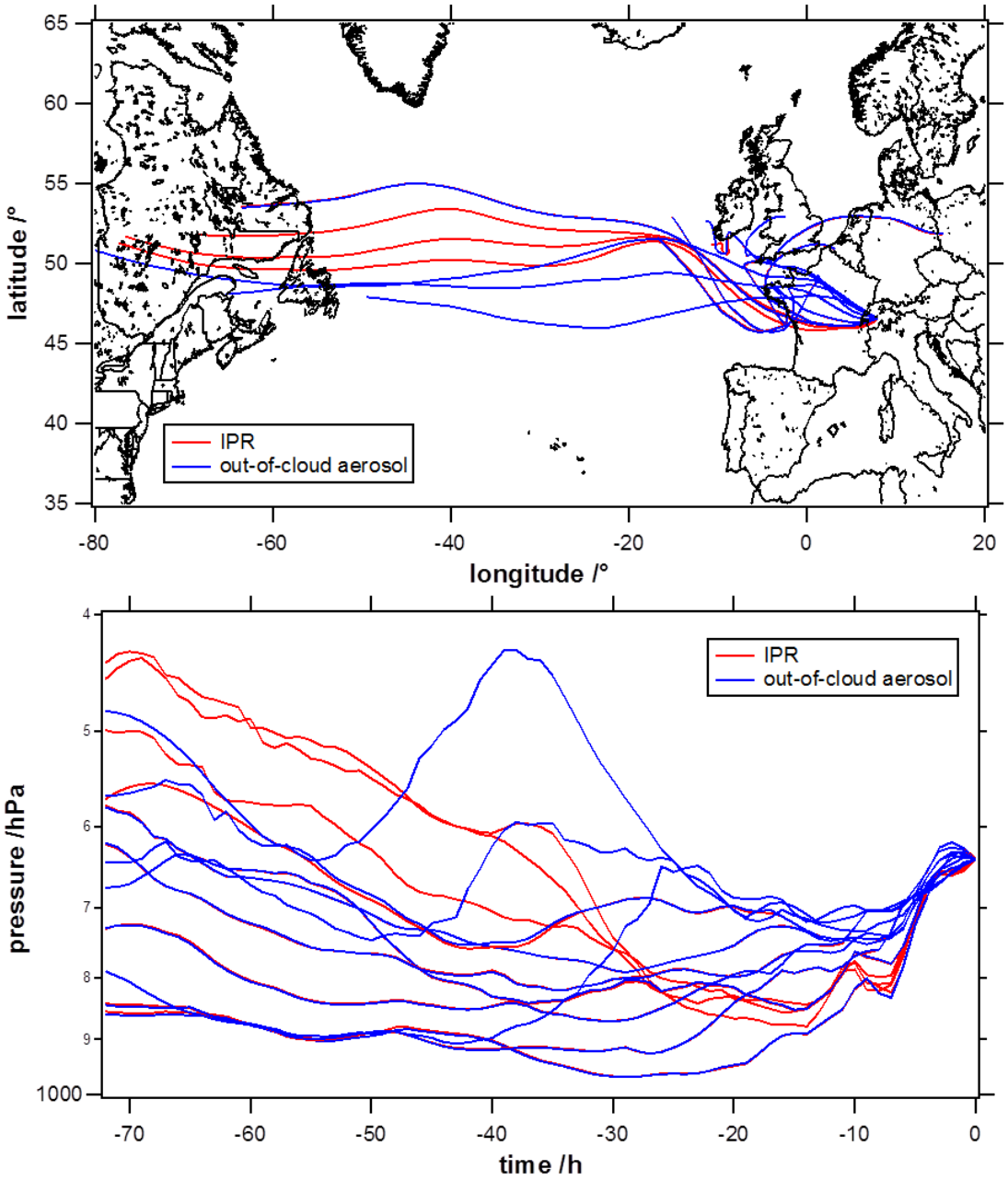

Fig. 6: Back trajectories (above) and air mass pressure as a function of time (below) for both sampling periods (red: IPR; blue: out-of-cloud aerosol).

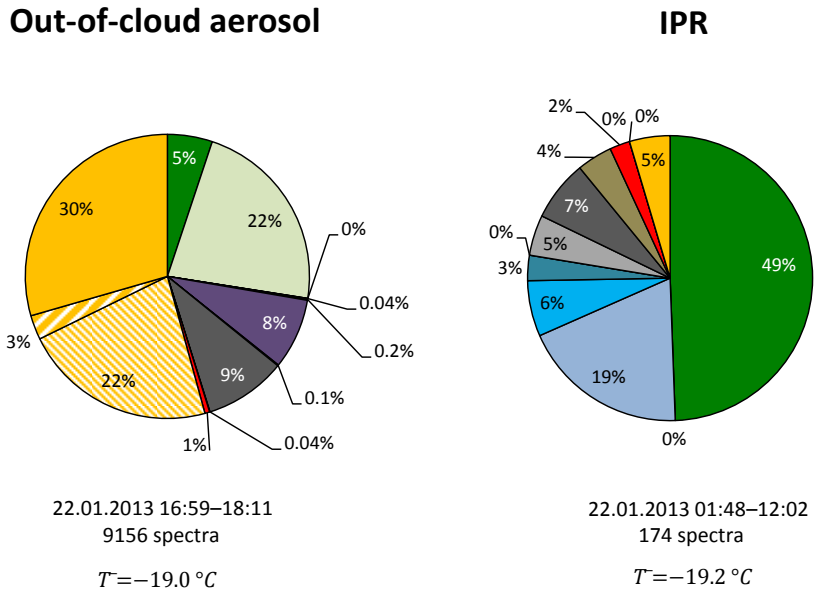

22.01.2013 16:59–18:11
9156 spectra

$T^- = -19.0\ °C$

22.01.2013 01:48–12:02
174 spectra

$T^- = -19.2\ °C$

Particle type	Out-of-cloud		IPR		% IPR / % Out-of-cloud
	Total number	percentage	Total number	percentage	
biological/amine	469 (± 74)	5.1 (± 0.8)%	86 (± 36)	49 (± 20) %	9.6 (± 4.3)
biomass burning	2047 (± 310)	22.3 (± 3.4)%	0	0	0
soil dust	0	0	33 (± 14)	19.0 (±8.2) %	--
minerals	4 (± 2)	0.04 (± 0.02)%	11 (± 6)	6.3 (± 3.2)%	150 (± 100)
sea salt/cooking emissions	16 (± 5)	0.17 (± 0.05)%	5 (± 3)	2.9 (± 1.7) %	16 (±11)
aged material	735 (± 114)	8.0 (± 1.2)%	0	0	0
engine exhaust	10 (± 4)	0.1 (± 0.04) %	8 (± 4)	4.6 (± 2.4) %	42 (± 27)
PAH/soot	853 (± 131)	9.3 (± 1.4)%	12 (± 6)	6.9 (± 3.4) %	0.7 (± 0.4)
lead-containing	4 (± 2)	0.04 (± 0.02)%	7 (± 4)	4.0 (± 2.2) %	92 (± 70)
industrial metals	50 (± 10)	0.54 (± 0.11) %	4 (± 2)	2.3 (± 1.2) %	4.2 (± 2.3)
K dominated	2016 (± 306)	22.0 (± 3.3) %	0	0	0
Na + K	254 (± 41)	2.8 (± 0.45) %	0	0	0
others	2698 (± 408)	29.4 (± 4.5) %	8 (± 4)	4.6 (± 2.4) %	0.15 (± 0.08)

Fig. 7: Comparison of the abundance of particles types in out-of-cloud aerosol (left) and the IPR (right) ~~chemical composition~~ at similar sampling conditions during each sampling period of. The table lists absolute number of particles with uncertainties, percentages, and "enrichment factor" (percentage IPR / percentage out-of-cloud).